

**MAGMA MIXING
IN THE POST-GLACIAL VEIDIVÖTN FISSURE ERUPTION,
SOUTH-EAST ICELAND**

A microprobe study of mineral and glass variations

by

Mai Britt E. Mörk

1 9 8 2

NORDIC VOLCANOLOGICAL INSTITUTE 8205
UNIVERSITY OF ICELAND

**MAGMA MIXING
IN THE POST-GLACIAL VEIDIVÖTN FISSURE ERUPTION,
SOUTH-EAST ICELAND**

A microprobe study of mineral and glass variations

by

Mai Britt E. Mörk

1 9 8 2

ABSTRACT

Local tephrastratigraphy and chemical analyses of lavas and tephras provide detailed information on the eruptive history of the mixed post-glacial Veidivötn fissure eruption. The continuous chemical variation of the glasses from basalt to rhyolite is interpreted as a result of magma mixing. Phenocrysts from the basaltic and rhyolitic end member magmas are frequently distributed throughout the suite of mixed rocks, and are used as tracers to study the mixing.

The basaltic magma intruded into the rhyolitic magma chamber shortly before the eruption. The effects of this intrusion were: (1) Rapid mixing with formation of small volumes of homogeneous intermediate melts (heterogeneous at a larger scale) in the contact area of the rhyolitic magma chamber. These silicic melts were extruded shortly after the mixing in the first phase of explosive, mixed tephra eruptions. (2) The main volume of the rhyolitic magma erupted as lavas at a later stage. The basalt intrusion here resulted in contamination of the rhyolite in part by complete mixing and in part by chilling of the basalt (1140°C) against the colder rhyolite melt (900°C), as evidenced by the numerous partly dissolved xenoliths and xenocrysts in the lavas. (3) Resorption and partial reequilibration (zoning) of the original phenocrysts in response to the changing melt chemistry and temperature variations during magma mixing.

INTRODUCTION

The Veidivötn fissure in the south-eastern volcanic zone of Iceland erupted tephras and lavas ranging from basalt to rhyolite simultaneously during a single post-glacial event (Sæmundsson 1972, Larsen 1978). The over 35 km long crater row produced mainly basaltic tephra (Larsen 1980). Silicic and mixed products were erupted in the southern part of the fissure where it extends into the Torfajökull silicic center (Fig. 1). It was suggested by Sigurdsson (1970) and Jakobsson (1979) from a few lava analyses that the acid and basic rocks were unlikely to be related genetically. Sr-isotope studies from the simultaneously erupted Námshraun and Stútshraun lavas (O'Nions & Grönvold 1973) show higher $^{87}\text{Sr}/^{86}\text{Sr}$ -values for the acid lavas than for the basalt, ruling out any direct genetic relationships.

The present study involves both the tephras and the lavas, and the purpose is to look at the mixed eruption products in detail chemically and mineralogically. From the glassy state of the tephras and lavas, and from the chemistry of phenocrysts, detailed information is obtained on the state of the magma at eruption and thereby on the scale and extent of the mixing process. The tephra stratigraphy (from Larsen in prep.) also allows some deductions of the time sequence to be obtained.

The obsidian flows, Laugahraun and Námshraun, were produced in the southernmost eruption craters (Fig. 1) of the Veidivötn fissure while the Stútshraun and Ljótípollur craters further north produced the basaltic lavas. In addition considerable amounts of tephra erupted in the Námshraun, Stútshraun and Ljótípollur craters. The volcanic activity in these craters is all part of the same eruption, and this activity was simultaneous with the basaltic eruptions in the Veidivötn crater row further north along the fissure (Larsen in prep.). The time sequence of eruption and the relative emplacement of lava



Fig. 1a.
The neovolcanic zone in Iceland with main fissure swarms. The position of the Veidivötn volcanic line is marked by the arrow.

Fig. 1b.
The Veidivötn and the older Vatnaöldur volcanic line, transecting the Torfajökull silicic Complex (Central volcano). The map is simplified after Kjartansson (1962), showing the main tephocraters and lavas. Inlet gives the position of the more detailed sampling map (Fig. 2).



and tephra is illustrated in the simplified tephra profiles (Fig. 3).

According to Larsen (in prep.) the volcanic activity of the four southernmost eruption sites began with an explosive phase of short duration. The first material to appear was yellow to white non-juvenile tephra ("mud") at the Laugahraun area, indicated in the tephra profiles (Fig. 3) as base layer. Shortly thereafter explosive activity with tephra eruption began at the Námshraun and Stútshraun craters. This was followed by an effusive

phase which produced the four lavas shown in Fig. 2.

To cover the total compositional range of the erupted melts both lavas and tephra were sampled (sampling locations on Figs. 2, 3). The tephra samples include both bulk samples representing the various layers and selected clasts to cover the total colour variations recorded in the tephra. The rhyolitic lavas were sampled for microprobe analyses of glassy matrix and for xenoliths, while the more crystalline basaltic lavas are represented only by whole rock analyses (Table 1).

Sampling locations

Námshraun tephra N1-N5 was sampled in a 1 m thick profile near the largest Námshraun crater. Stútshraun tephra was sampled in four places: S1-S6 represent a 1 m thick profile in a road cut in the southeastern corner of the Stútshraun crater. The two samples SØ1 and SØ2 were collected from the northeastern crater wall to supplement the S3 horizon. S7 is from a road cut near the top of the western crater rim and S8 is collected near the foot of the Stútur nested scoria cone inside the crater. Ljótipollur tephra Lj1 and Lj2 was sampled near the crater lake in the northwestern part of the crater and Lj3 under the welded layer near the top of the crater. In addition to the locations shown in Fig. 2 basaltic tephra from Veidivötn, about 10 km further north along the fissure, is included in the study to examine chemical variation away from the Torfajökull silicic complex.

Analytical procedure

Chemical analyses of minerals, natural glasses and fused samples were performed on an ARL SEMQ fully automated crystal dispersive microprobe at the Nordic Volcanological Institute, Reykjavik. Glassy matrix of the tephra and the

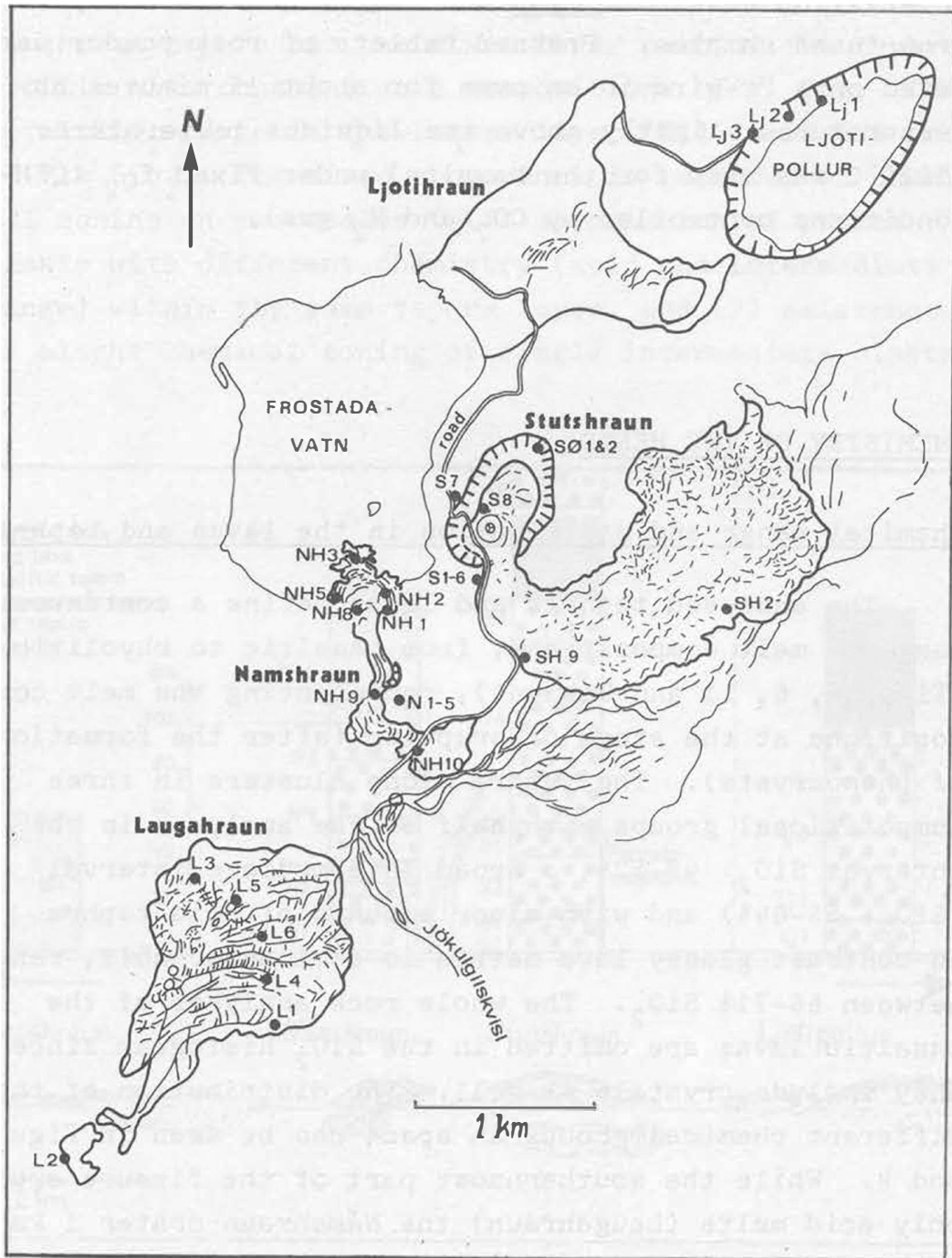


Fig. 2.

Sampling map of the southern part of the Veidivötn fissure, with lavas and tephra craters drawn from air photos. Descriptions of sampling locations in the text.

acid lavas was analysed directly on the microprobe; the acid and intermediate glasses with a slightly unfocused beam and moving sample to prevent alkali loss. The more crystalline basaltic lavas and xenoliths were analysed from fused samples. Pressed tablets of rock powder were fused on a Pt-wire in an oven for about 15 minutes at temperatures slightly above the liquidus temperatures (1220°C was used for the basalts) under fixed f_{O_2} (QFM-conditions controlled by CO_2 and H_2 gas).

CHEMISTRY OF THE MELTS

Chemical range and distribution in the lavas and teph \underline{r} as

The analysed teph \underline{r} as and lavas define a continuous range of melt compositions, from basaltic to rhyolitic (Figs. 4, 6, 11 and Table 1), representing the melt compositions at the stage of eruption (after the formation of phenocrysts). The teph \underline{r} a alone clusters in three compositional groups with half of the analyses in the interval SiO_2 : 48-52%, a broad intermediate interval (SiO_2 : 55-64%) and with minor amounts of acid teph \underline{r} a. In contrast glassy lava matrix is dominantly acid, ranging between 66-71% SiO_2 . The whole rock analyses of the basaltic lavas are omitted in the SiO_2 histogram since they include crystals as well. The distribution of the different chemical groups in space can be seen in Figs 3 and 4. While the southernmost part of the fissure erupted only acid melts (Laugahraun) the Námshraun crater 1 km to the north erupted both acid and intermediate melts and the Stútshraun crater erupted dominantly basaltic melts with minor intermediate and acid melts. The Ljótípollur crater further north erupted only basaltic melts. There is thus a regional decrease in the rhyolitic component northwards along the eruptive fissure.

Chemical evolution during eruption

Námshraun eruption site

Intermediate compositions are most common in the Námshraun tephra but the mixed lower part of the tephra profile also contains acid compositions (Fig. 3b). The total SiO_2 -range in the lowest layer (N1) is 55-64% and 67-71% SiO_2 . The mixed appearance is recorded as chemical zoning on two scales: (1) association of pumice clasts with different chemistry (acid and intermediate range) within the same tephra layer, and (2) existence of slight chemical zoning of single intermediate clasts.

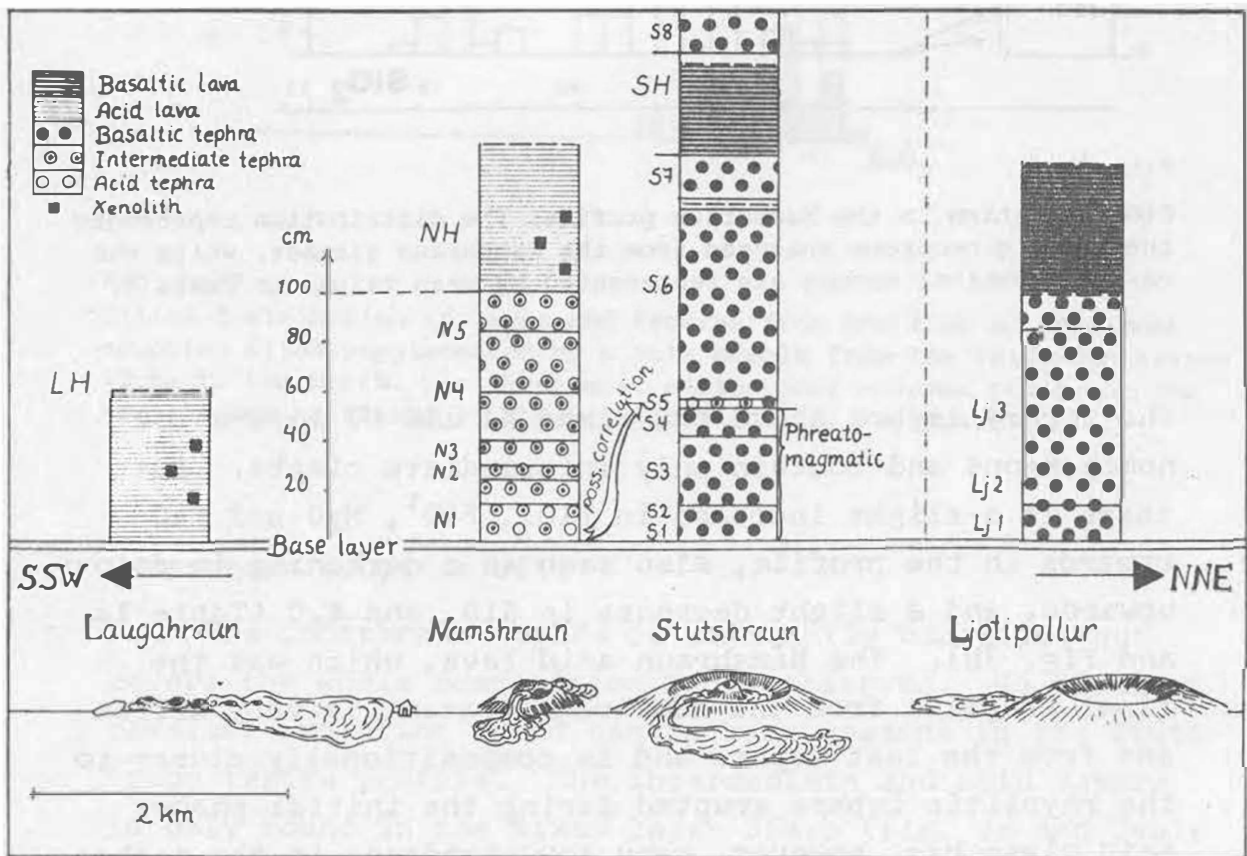


Fig. 3a.

Sampling stratigraphy for the Laugahraun, Namshraun, Stutshraun and Ljotipollur eruption sites, showing the distribution of and order of eruption of lavas and tephras. The eruption products are divided into three compositional groups: acid, intermediate and basic. The vertical scale of tephra profiles is only valid for the Namshraun and Stutshraun profiles.

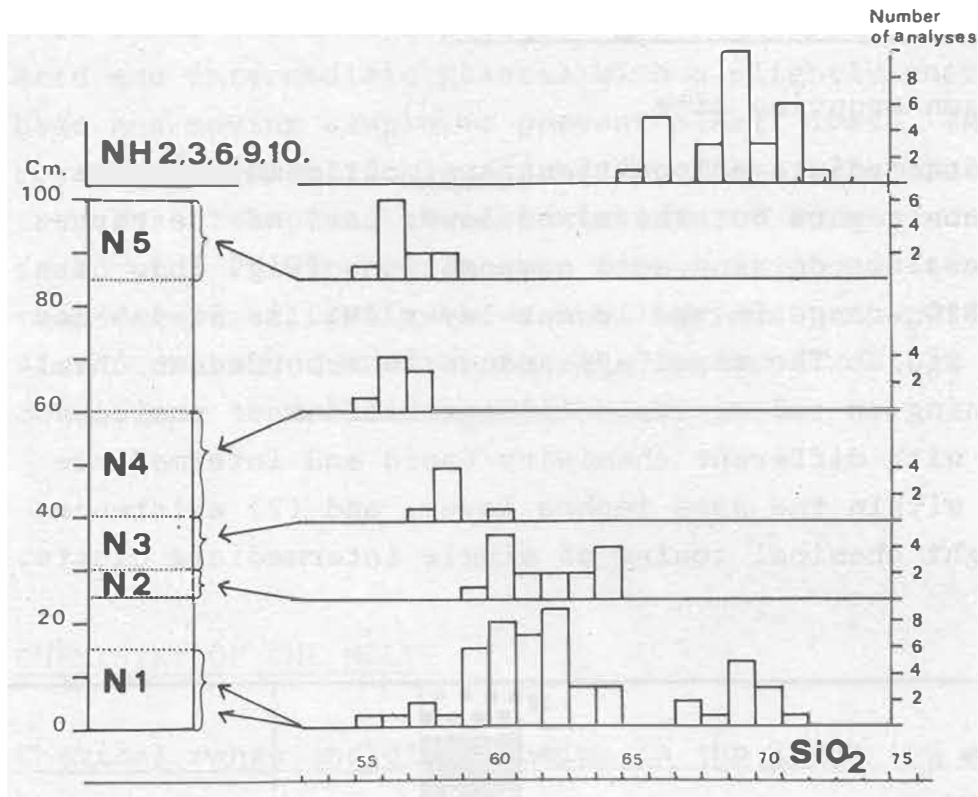


Fig. 3b.

SiO₂-variation in the Namshraun profile. The distribution represents the total microprobe analyses from the Namshraun glasses, while the various chemical groups are represented by mean values in Table 1.

The tephra layers above the mixed N1 and N2 layers are homogeneous and contain only intermediate clasts. But there is a slight increase in TiO₂, FeO^t, MgO and CaO upwards in the profile, also seen as a darkening in colour upwards, and a slight decrease in SiO₂ and K₂O (Table 1a and Fig. 3b). The Námshraun acid lava, which was the final eruption from the Námshraun crater, is very different from the last tephra and is compositionally closer to the rhyolitic tephra erupted during the initial phase. Acid glass has, however, very low abundance in the tephra.

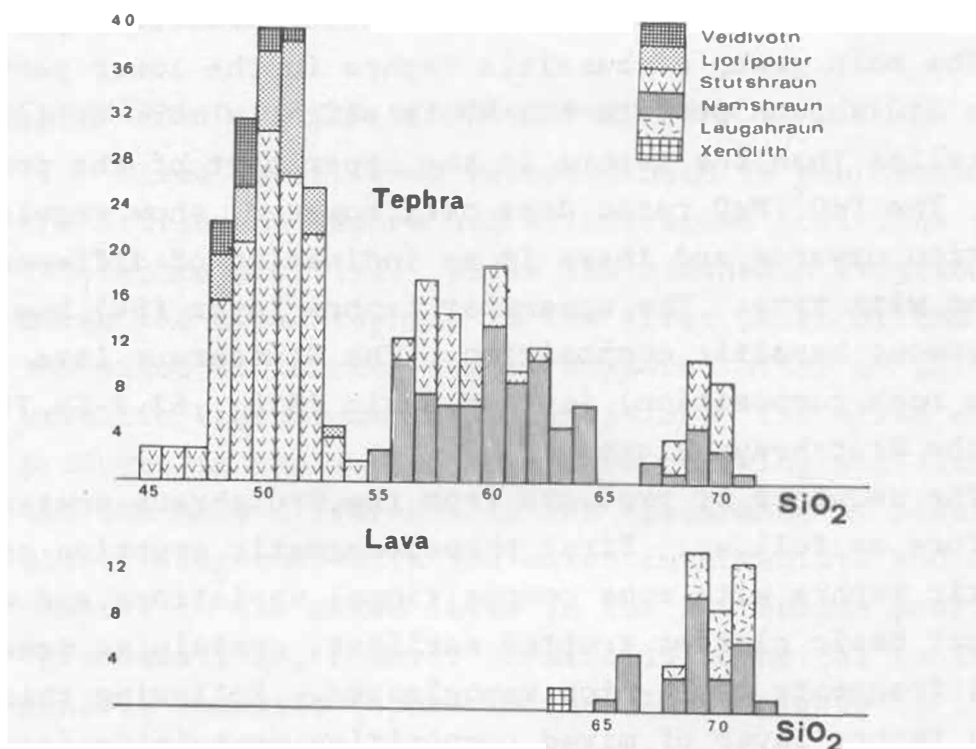


Fig. 4.
Silica distribution in lavas and tephra from the four southernmost eruption sites supplemented by a bulk sample from the Veidivötn crater 10 km to the north. The three most silica-poor columns represent the xenoglasses mentioned in the text (high-Ti, P, Fe basalt).

Stútshraun eruption site

The Stútshraun tephra is dominantly basaltic, but covers the whole composition range observed. No distinct chemical evolution trend can be seen upwards in the Stútshraun tephra profile. The intermediate and acid tephra is only found in the mixed layer S5a,b (Fig. 3a and Table 1a) which constitutes only a few cm thick horizon. This layer separates the homogeneous upper part of the tephra profile from the lower phreatomagmatic, heterogeneous part. According to Larsen (in prep.) there is a hiatus between the phreatomagmatic phase and the mixed silicic layer, but with no significant time span. The lower

heterogeneous part of the profile contains gravel and also basaltic xenoglasses with characteristic high contents of Ti, Fe and P in addition to the juvenile basaltic tephra.

The main group of basaltic tephra in the lower part of the Stútshraun profile (S1-4) is slightly more enriched in alkalis than the tephra in the upper part of the profile. The $\text{FeO}^{\text{t}}/\text{MgO}$ ratio does not, however, show regular variation upwards and there is no indication of differentiation with time. The uppermost tephra layer (S8) has a homogeneous basaltic composition. The Stútshraun lava (whole rock composition) is less basic (SiO_2 : 53.3-54.7%) than the Stútshraun glasses.

The sequence of products from the Stútshraun crater is therefore as follows: First phreatomagmatic eruption of basaltic tephra with some compositional variations and with the most basic glasses erupted earliest, containing occasional fragments of Ti-rich xenoglasses. Following this is a thin tephra layer of mixed composition containing intermediate, acid and basaltic glasses terminated by basaltic tephra without xenoglasses. The next phase of the eruption is the Stútshraun lava which is slightly more silicic although close to basalt. Finally basaltic tephra was erupted forming the Stútur cinder cone.

Ljótípollur and Veidivötn eruption sites

The Ljótípollur crater produced only basaltic tephra and lava showing a small but significant chemical variation, and shows the same pattern as the Stútshraun crater with K_2O enrichment of the earliest erupted tephra. The sample collected from the top of the crater (Lj3) is less differentiated with lower SiO_2 , $\text{FeO}^{\text{t}}/\text{MgO}$ and K_2O than the two samples from the bottom of the crater (stratigraphically lower).

The Veidivötn crater row was not studied in detail, but a random tephra sample shows a homogeneous basaltic

composition and has the least differentiated chemistry of all the samples studied.

Correlation of the eruption sequences

Mixed layers were recorded both in the Námshraun and the Stútshraun tephra but at different positions in the two tephra profiles. While the Námshraun eruption produced the mixed tephras in the first phase of the eruption, the mixed Stútshraun tephra appeared after an initial basaltic (phreatomagmatic) eruption. The mixed eruption products in the two craters have striking similarities, and the only difference is the appearance of basaltic clasts (together with the mixed intermediate and acid clasts) in the mixed layer in the Stútshraun profile. This basalt is, however chemically identical to the homogeneous basaltic tephra in the layers higher up in the profile.

Since the appearance of mixed and chemically zoned clasts is similar to the Námshraun mixed tephra, it is tempting to correlate S5a,b with N1 and N2. If all the intermediate and acid tephra were erupted from the Námshraun crater, the phreatomagmatic basaltic part of the Stútshraun eruption would either be earlier or simultaneous with the first phase of the Námshraun eruption. This would mean that the Stútshraun crater was erupting basalt before the Námshraun crater erupted mixed silicic tephra. The other alternative, that the Stútshraun crater erupted the mixed silicic S5 tephra, requires that silicic melts either were stored at different places under the volcanic line, or that minor melts from the acid magma chamber were brought to the Stútshraun eruption site along with the more voluminous basaltic magmas. Anyhow, the composition of the Stútshraun lava shows that this crater erupted mixed melts at a later stage.

In either case the S5 layer in the Stútshraun profile marks a change in the eruption from phreatomagmatic to mag-

matic coinciding with a chemical change with slight decrease in alkali content. The last phase with homogeneous basaltic tephra in the Stútshraun and Ljótípollur eruptions is very similar to the tephra erupted from the Veidivötn crater, with characteristically low K_2O values. The earliest basalts erupted are the most heterogeneous with slight variations towards higher alkali content than in the latest erupted basaltic tephra. There is therefore a positive correlation between explosivity of eruption and alkali content, as suggested elsewhere (Jakobsson 1979).

Acid lavas and basaltic xenoliths

The glass phase of the Laugahraun lava is almost homogeneous chemically (composition range SiO_2 : 69.2-71.5%) while the glass composition in the more heterogeneous Námshraun lava ranges between 66-71.5% SiO_2 (Table 1b). The flow-layering recorded in both lavas has, however, not revealed any chemical difference. Wetzel et al. (1978) explained chemical variation in various obsidian flows in the Torfajökull area by contamination from basaltic xenoliths. This contamination hypothesis is supported by the present findings, and is further interpreted as part of the large-scale magma mixing involving the tephra products as well. The xenoliths are described in more detail in order to illustrate the contamination process.

Xenoliths are common both in the Laugahraun and in the Námshraun acid lava, usually in rounded or elongated shapes of 1-2 cm length, but ranging in size between a few mm and a dm. The xenoliths contain the same type of glomerocrysts as recorded in the basaltic tephtras (described later). The xenolith matrix is, however, slightly more crystalline than the matrix of the tephtras and of the acid lavas, and is crowded with minute crystallites with only very restricted domains of glass. Homogeneous glass without crystals or with radially oriented plagioclase laths often

forms a rim around the xenoliths, and grades into the lava matrix which is more crowded with plagioclase microlites.

Detailed chemical studies of the lava matrix revealed no chemical gradients on the mm-scale or the cm-scale towards xenolith contacts. However, small glassy domains within the xenolith NH3 have a slightly more silicic chemistry (63% SiO₂) than the xenolith whole rock analysis, while the surrounding lava matrix contains 66% SiO₂. The homogeneous glass rim around the xenolith is chemically similar to the lava matrix outside it.

Generally the least silicic glasses in the lavas are recorded in the samples which contain the larger xenoliths, suggesting that these compositions are the most contaminated melts. For example, the basaltic xenolith NH1, which is the largest of the xenoliths studied, (largest axis 9 cm) is rimmed by an irregular zone (up to 2 cm thick) of homogeneous vesicular glass of composition 67.6% SiO₂. On the other hand the appearance of both intermediate and basaltic xenoliths that contain the same type of basaltic glomerocrysts suggests that the xenoliths are contaminated by the acid melt as well. The xenolith NH3 with intermediate glass domains is texturally gradational with the lava matrix.

Were the xenoliths incorporated in the rhyolitic magma in a solid or a liquid condition? The basaltic glomerocrysts were present before the incorporation into the rhyolitic magma, where they occur as xenocrysts in all parts of the lavas. Textural and mineral-chemical considerations (to be discussed later) show that the basaltic xenocrysts have the same source as the xenoliths. Dark colouring of the lava matrix around many xenocrysts and xenocryst aggregates, and the variable xenocryst appearance, ranging from isolated crystals to glomerocrysts and xenolith aggregates, demonstrates that the basaltic component was dissolved into the acid melt. Twisted xenolith appearance and dark coloured spots with acid compositions forming pseudomorphs of dragged-out xenoliths suggest incorporation of the basaltic component while in the liquid

state, thus mixing of basaltic and rhyolitic magmas. Lack of chemical gradients at the xenolith lava contacts and across the dark coloured lava domains mentioned above means that the mixing and dissolution process was associated with rapid turbulence/flow which resulted in homogenization of the magma in local domains. The basaltic xenoliths may have formed by quenching of the basaltic magma when intruded into the rhyolitic magma chamber as described from other places (Sparks et al. 1977, Sigvaldason 1979). Rapid cooling of the basalt therefore sometimes prevented complete mixing. Due to the high abundance of xenoliths, various degrees of contamination can be expected in all parts of the acid lavas, making it difficult to define the original acid liquid composition.

Products of the magma mixing

The products of the mixing appear as homogeneous tephra fragments and lava matrix and also as heterogeneous and more crystalline xenoliths in the lavas. The almost continuous range of melt compositions shows that mixing has occurred in various proportions between the two end members. The close association of these different melt products is recorded as: (a) more or less regular variations upwards in the tephra, suggesting that the extent and character of the mixing was either changing with time or with position in the magma reservoir, (b) single mixed tephra layers dominated by intermediate compositions and with minor amounts of glasses representing the end component compositions, (c) pumice clasts with chemical layering demonstrating the close association of intermediate mixing products resulting from slightly different proportions of the end components.

In the composite clasts the different melts are chemically homogeneous on the mm scale and up to a few cm. Homogeneous clasts on the dm scale are recorded in the mixed tephra horizons, and homogeneous intermediate tephra layers define large volumes of complete mixing in the Námshraun

tephra.

The acid lavas, generally homogeneous at least on the scale of a thin section, are also mixed and the abundant xenoliths are relicts of a basaltic contaminant in these lavas. The most contaminated acid glass is found in the Námshraun lava, close to xenoliths.

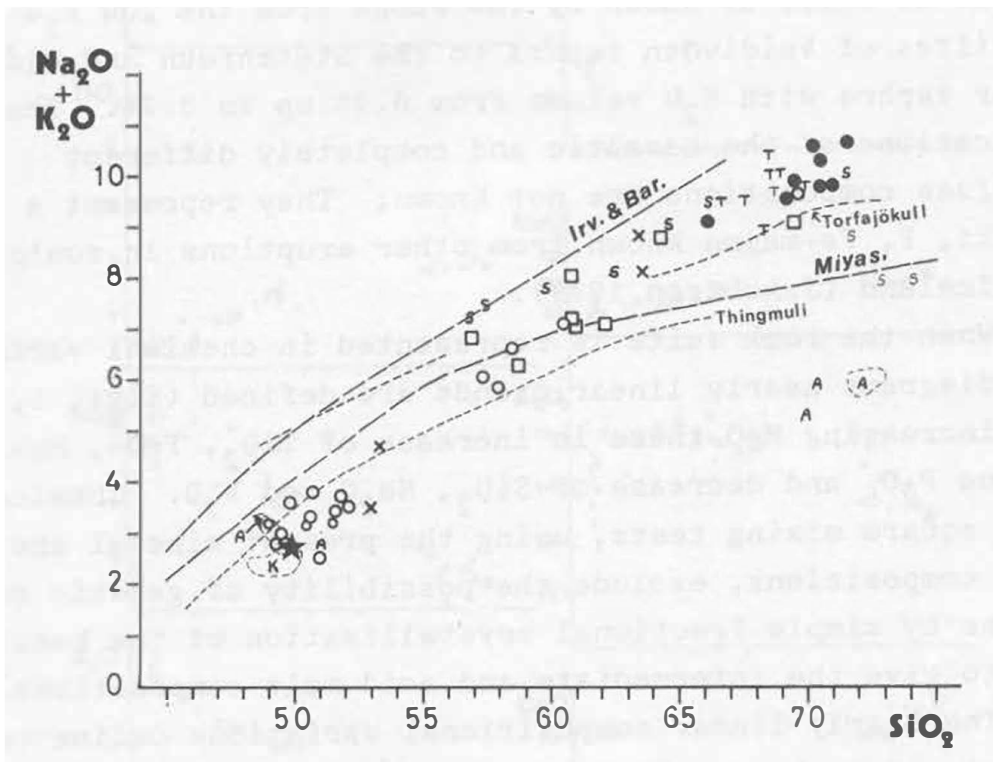


Fig. 5. Alkali - silica plot of mean values of glass compositions (Table 1). Dividing lines after Irvine & Baragar (1971) and Miyashiro (1978). Also shown are alkaline acid rocks from the Setberg (S) and Torfajökull (T) regions (Sigurdsson 1970) and tholeiites from Krafla (K) (Grönvold & Mäkipää 1978) and tholeiites and dacites from Askja (A) (Sigvaldasson 1979). The established trends are based on whole rock analyses and the comparisons with the few glass analyses available (A) & (K) are therefore most appropriate. Symbols: ● Acid lavas (Laugahraun and Namshraun). □ Namshraun tephra. ○ Stutshraun tephra. o Ljotipollur tephra. ★ Veidivötn tephra. X Xenoliths.

Chemical variation and problems of end members

The suite of eruption products is compared with other Icelandic eruption series in Fig. 5. The basaltic eruption products classify as tholeiite; the acid lavas have a slightly more alkaline character (but are still close to rhyolite) while the intermediate glasses are transitional with respect to alkalinity (Fig. 5). At a finer scale potassium variations are significant in the basaltic tephra as well, as shown by the range from the low K_2O tholeiites of Veidivötn tephra to the Stútshraun and Ljótípollur tephra with K_2O values from 0.3% up to 0.7%. The implications of the basaltic and completely different xenoglass compositions are not known; They represent a high-Ti, P, Fe-magma known from other eruptions in south-east Iceland (Jakobsson 1979).

When the rock suite is represented in chemical variation diagrams nearly linear trends are defined (Figs. 5, 6). With increasing MgO there is increase of TiO_2 , FeO^t , MnO, CaO and P_2O_5 and decrease of SiO_2 , Na_2O and K_2O . Chemical least square mixing tests, using the present mineral and glass compositions, exclude the possibility of genetic relations by simple fractional crystallization of the basaltic melt to give the intermediate and acid melt compositions.

The nearly linear compositional variations define two obvious end members: The most acidic and the most basic of the glasses. But simple mixing of the two end member compositions is not sufficient to form the chemical pattern seen. The most pronounced deviation from linearity in the variation diagrams for the glasses can be seen for the elements Al, Ca, and Na, and especially the Al values show great irregularities in the acid lavas. These deviations might be caused by plagioclase crystallization with the widespread formation of plagioclase microlites at a late stage. As will be evident from the section on mineralogy, the resorption of phenocrysts is another type of mineral contribution in the mixing process since plagioclase resorption would cause Al increase in the mixed melts.

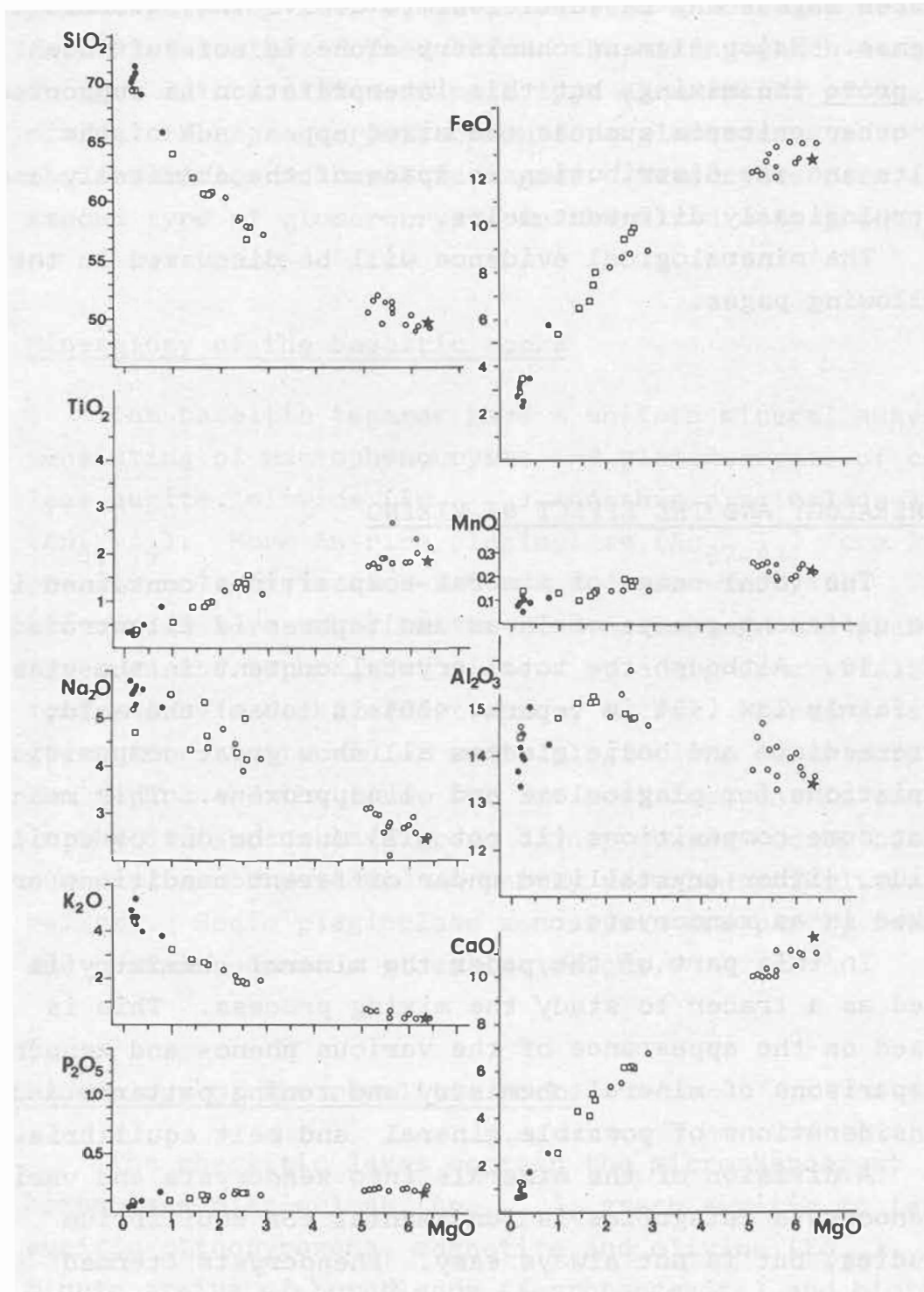


Fig. 6.
MgO-oxide variation diagrams, with symbols as in Fig. 5.

Mixing involving both minerals and basic and acid end member magmas may be sufficient to derive the intermediate magmas. Major element chemistry alone is not sufficient to prove the mixing, but this interpretation is supported by other criteria such as the mixed appearance of the melts and the distribution in space of the chemically and petrologically different melts.

The mineralogical evidence will be discussed in the following pages.

MINERALOGY AND THE EFFECT OF MIXING

The total range of mineral compositions contained in the different groups of lavas and tephras is illustrated in Fig. 10. Although the total crystal content in the glasses is fairly low (<5% in tephra, <20% in lavas) the acid, intermediate and basic glasses all show great compositional variations for plagioclase and clinopyroxene. This means that some compositions (if not all) must be out of equilibrium, either crystallized under different conditions or mixed in as xenocrysts.

In this part of the paper the mineral chemistry is used as a tracer to study the mixing process. This is based on the appearance of the various pheno- and xenocrysts, comparisons of mineral chemistry and zoning patterns and considerations of possible mineral and melt equilibria.

A division of the minerals into xenocrysts and various phenocrysts categories is fundamental for equilibrium studies, but is not always easy. Phenocrysts (termed microphenocrysts when <0.3 mm) may have formed in the melt early, while microlites possibly formed in the final cooling stage and are most likely to be in equilibrium with the glass. But the importance of size is not always clear. For example in the acid lava plagioclase varies continuously

in size from microlites to microphenocrysts and to larger phenocrysts (up to 1/2 mm). The term xenocrysts is used for crystals that formed before the mixing which were brought into a different melt type as a result of magma mixing. The phenocrysts often form glomerocrysts both in the rhyolitic and basaltic magmas. Xenocrysts form a second type of glomerocrysts in the mixed melt products.

Mineralogy of the basaltic rocks

The basaltic tephra have a uniform mineral assemblage consisting of microphenocrysts and glomerocrysts of colourless augite, olivine (Fo_{74-79}) and thin plagioclase laths (An_{66-79}). More An-rich plagioclase (An_{87-83}) form larger pheno(xeno?)crysts (0.5-0.8 mm) and glomerocrysts. The Stútshraun lava contains the same assemblage and phenocryst types as the tephra, but differs by a higher crystal content and by a dark, almost opaque matrix. Xenocrysts of green ferroaugite and of sodic plagioclase occur both in the tephra and the lava, but are most frequent in the lava. In the Stútshraun lava green clinopyroxene occurs both as euhedral xenocrysts and as partly resorbed poikilitic relicts. Sodic plagioclase xenocrysts are partly resorbed and contain numerous glass inclusions.

Mineralogy of the rhyolitic rocks

The rhyolitic lavas contain the microphenocryst assemblage plagioclase (An_{15-27}), green augitic to ferroaugitic clinopyroxene, magnetite and olivine (Fo_{20}). Minute grains of hornblende (ferropargasite) and biotite were recorded in two samples. The size range for the phenocrysts is: oligoclase, 0.5-2.0 mm, clinopyroxene, 0.2-0.8 mm, magnetite, 0.05-0.4 mm. These phases often form glomerocrysts with different crystal size combinations. Together with the mutual inclusion relationships

between oligoclase, clinopyroxene and magnetite this demonstrates simultaneous crystallization of the three phases. Olivine is rare and has a branching appearance. Plagioclase microlites are wide-spread in the acid lava matrix, and often oriented with parallel alignment. These are likely to have formed after the glomerocrysts during ascent of the lava.

In the few samples of acid tephra examined, crystals are scarcer than in any other glasses, but phenocrysts of oligoclase and green clinopyroxene were found.

In the acid lavas xenocrysts of colourless clinopyroxene, olivine (Fo_{66-77}) and plagioclase (An_{51-74}) are abundant both as glomerocrysts and as isolated crystals (<0.1-0.4 mm size). These crystals are distinguished from the lava phenocrysts by mineral chemistry and by crystal shape.

The basaltic to intermediate xenoliths in the acid lavas have the same mineral textures and mineral chemistry as the xenocrysts (Fig. 10). It was earlier argued that the xenocrysts and the xenoliths could both be relicts of the same basaltic magma component. They can also be comparable with the phenocrysts in the basaltic eruption products.

Mineralogy of the intermediate rocks

The intermediate tephra contains both the basaltic and the rhyolitic phenocryst types and assemblages. Basaltic glomerocrysts are most common, and are similar both texturally and chemically to those described in the basaltic tephra and to xenocrysts in the acid lavas. In addition the An-rich phenocryst type (bytownite) found in the basaltic glasses is also recorded in the intermediate tephra. Green clinopyroxene and oligoclase have the same appearance and chemistry as the phenocrysts in the acid lavas. Most of the crystals found in the intermediate glasses are therefore probably xenocrysts and inherited from the two end com-

ponent magmas. But the broad composition interval for plagioclase may indicate that at least some crystals were formed during the mixing as well. 12% of the plagioclase analyses fall in the range An_{52-63} which is not represented in the other melts.

Plagioclase variation in the basaltic melts

In the basaltic tephra the broad compositional interval for plagioclase (Figs 10, 12) reflects two generations of plagioclase: (1) Microphenocrysts in the basaltic tephra, occurring in glomerocrystals with olivine and clinopyroxene and as discrete laths, and (2) An-richer bytownite macrophenocrysts with pronounced zoning.

The macrophenocrysts are distinguished from the microphenocrysts by larger grain size, less elongated shapes, higher An content and zoning. The zoning is complex: the core region has weak zoning with An decreasing outward (An_{87-83}) or sometimes oscillatory zoning. In addition most crystals show abrupt An decrease in the rim, toward the same composition as the microphenocryst composition (An_{70}).

The Stútshraun lava, which has a slightly more evolved whole rock composition than the basaltic tephras, contains the same two types of basaltic plagioclase. The microphenocrysts show a chemical range from just over An_{70} to An_{50} with a dominant composition of about An_{67} . Bytownite macrophenocrysts (An_{87-80}) are more abundant and larger (up to 5 mm) than in the tephra but often with the same zoning pattern with outer rims compositionally similar to the microphenocrysts.

The distinct zoning pattern and the marked chemical contrast between the macro- and microphenocrysts indicates general disequilibrium between plagioclase and melt in the basaltic rocks. At least two growth stages of plagioclase are represented in the basalt. The compositional similari-

ties between the outer macrocryst rims and the microphenocrysts suggests that equilibrium is approached between plagioclase and the basaltic melt at this stage. The macrophenocrysts may represent either crystallization under different physical conditions, or the macrophenocryst cores may have formed from a more primary magma composition. A third possibility is that the macrophenocrysts are xenocrysts from a gabbroic crust.

Plagioclase variation in rhyolitic rocks

In the acid lavas the plagioclase phenocrysts show correlation between mineral fabric and degree of zoning. Three different phenocryst types are recognized texturally: (1) Euhedral to subhedral with sharp boundaries toward matrix, (2) subhedral to anhedral with seriate or rounded often diffuse boundaries, (3) partly resorbed crystals with "fingerprint texture" (Sigurdsson 1970) often located in a zone near the outer rim.

Type (1) phenocrysts are unzoned or only weakly and unsystematically zoned with An_{20} as mean rim composition. Type (2) have a distinct rimwards An increase (An_{18} - An_{20} , mean values) while the crystals with resorption textures (type 3) have the strongest An increase (An_{17} - An_{28} , mean values) with An_{42} as the most calcareous composition. The plagioclase domains with resorption textures are the most An rich, and these domains occur either in a thin zone close to the outer rim or in a broad zone including most of the crystal except the core.

The plagioclase microlites, which formed later than the phenocrysts, also show considerable chemical variation (An_{13-25}).

The microlites and the phenocrysts cover roughly the same composition interval. The phenocryst zoning together with the broad chemical composition interval for both plagioclase types therefore suggests that the magma was chemically heterogeneous during plagioclase crystallization.

The strong correlation between resorption textures and An increase in plagioclase phenocrysts is interpreted as evidence of magma mixing. The reversed zoning may be caused by two effects: (1) Heating effects when the basaltic magma comes into contact with the acid magma, (2) Change of magma composition due to mixing/contamination. Both processes may have influenced plagioclase chemistry in the present case. The very common An₂₀ composition may represent a late stage surface equilibrium. Heating effects may of course have occurred also prior to the main mixing and eruptive event, and the weak An increase may possibly reflect early heating. The most sodic plagioclase compositions were recorded in cores of the partly resorbed crystals. This may suggest that heating and magma contamination favoured plagioclase resorption in those crystals with the most metastable compositions.

Two types of plagioclase xenocrysts exist in the acid lavas. The most abundant type ranges between An₅₁₋₇₄ and occurs in "basaltic" glomerocrysts. The mean value, about An₇₀, is the same as the composition of the microphenocrysts in the basaltic tephra. The second type of plagioclase in the basalts, the zoned bytownite, is only recorded in the Námshraun lava in the least silicic sample (NH-3; dacite).

Plagioclase xenocrysts in the mixing products

In the intermediate tephra the composition range An₆₄₋₇₂ is most common among the microphenocryst laths. From the textures, mineral assemblages and chemistry they are interpreted to have formed in the basaltic melt before the final mixing stage, and are therefore xenocrysts. Larger bytownite crystals are common in the intermediate tephra. The characteristic zoning with an outer An₇₀ rim composition demonstrates that these crystals went through two stages of crystallization in basaltic melts, before the mixing.

Sodic plagioclase xenocrysts were recorded both in the intermediate tephra and in the Stútshraun basaltic (to intermediate) lava. Compositions near An_{50} form strongly resorbed xenocrysts in the Stútshraun lava showing the highest degree of dissolution into the melt. Since these crystals are more sodic than the microphenocrysts in the Stútshraun lava and are almost completely resorbed by the basaltic melt they might have reequilibrated from still more sodic compositions inherited from the acid magma.

Clinopyroxene variation and zoning

Clinopyroxene has formed green microphenocrysts in the rhyolitic melts and colourless microphenocrysts in the basaltic melts. The colourless type also occurs frequently as xenocrysts in the silicic and mixed eruption products. Both types have relatively low contents of TiO_2 , Al_2O_3 and Na_2O (Table 3). The green type is distinguished from the colourless by higher Fe/Mg ratio and a wider range of compositions in terms of Fe/Mg. The colourless clinopyroxene type has more restricted Fe/Mg variation with compositions above En_{40} and is termed "basaltic" clinopyroxene. Minor elements also separate the two groups with higher Mn and Na content in the green type and higher Ti and Al content in the basaltic clinopyroxene. However, some compositional gradations between the two clinopyroxene groups can be seen in the Mg-Fe-Ca diagram (Fig. 8). When all the analyses are considered the clinopyroxene compositions define an evolutionary trend opposite to normal differentiation trends (Fig. 8a). This evolution is interpreted in the following as a result of magma mixing.

The microphenocrysts in the acid lavas have a compositional range between En_{25-37} . The most pronounced zoning can be seen for Fe and Mg. The zoning is not systematic, but from the Mg-Fe-Al and Mg-Fe-Ca diagrams (Figs. 7, 8b) there seems to be a tendency toward increasing Mg/Fe con-

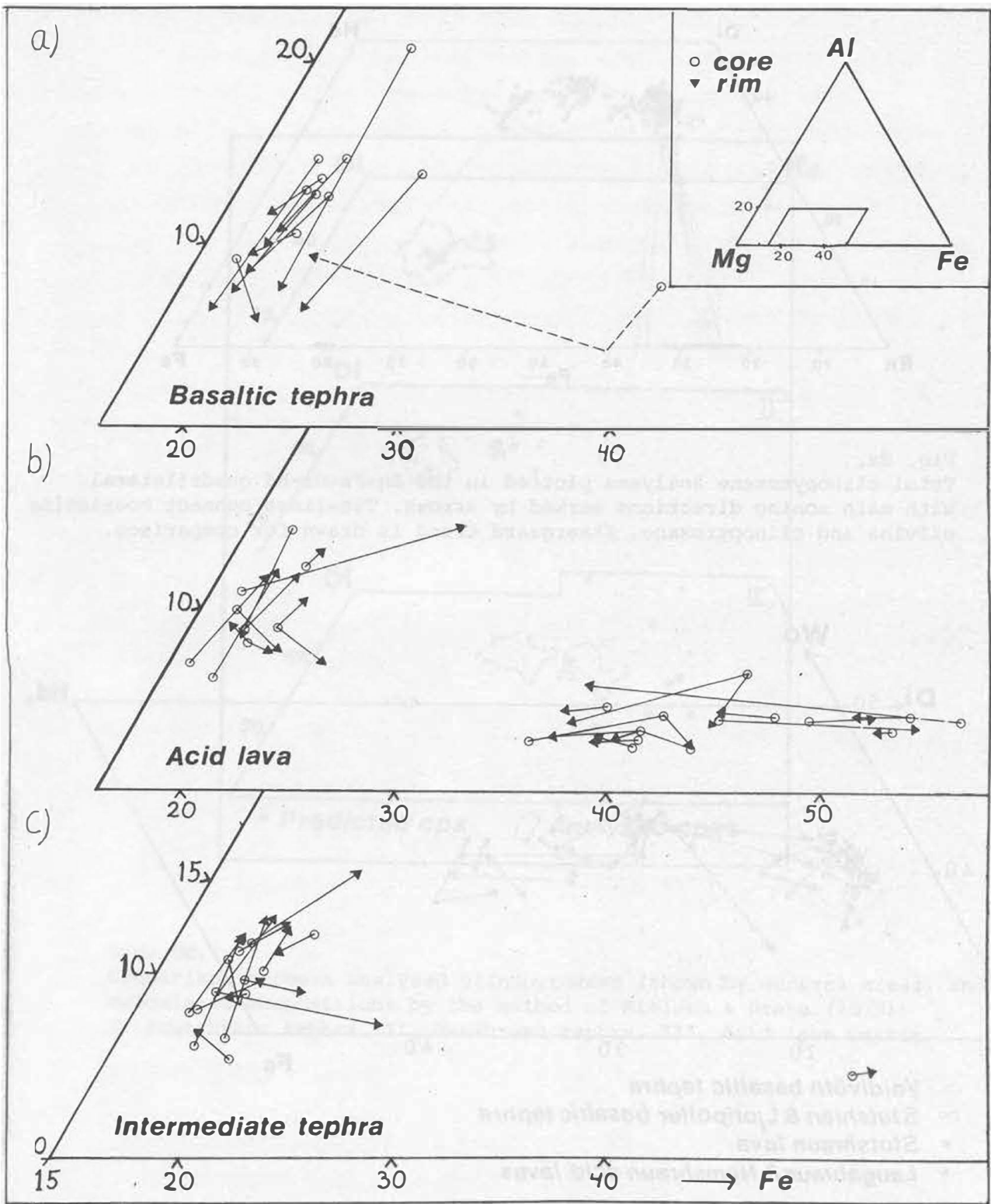


Fig. 7. Clinopyroxene zoning expressed by the components Mg-Al-Fe. Core and rim analyses are connected by arrows, pointing rimwards. (a) Stutshraun and Ljotipollur basaltic tephra (stippled arrow is a xenocryst). (b) Microphenocrysts in Laugahraun and Namshraun acid lavas (green cpx). Colourless xenocrysts are shown by stippled arrows. (c) Namshraun intermediate tephra.

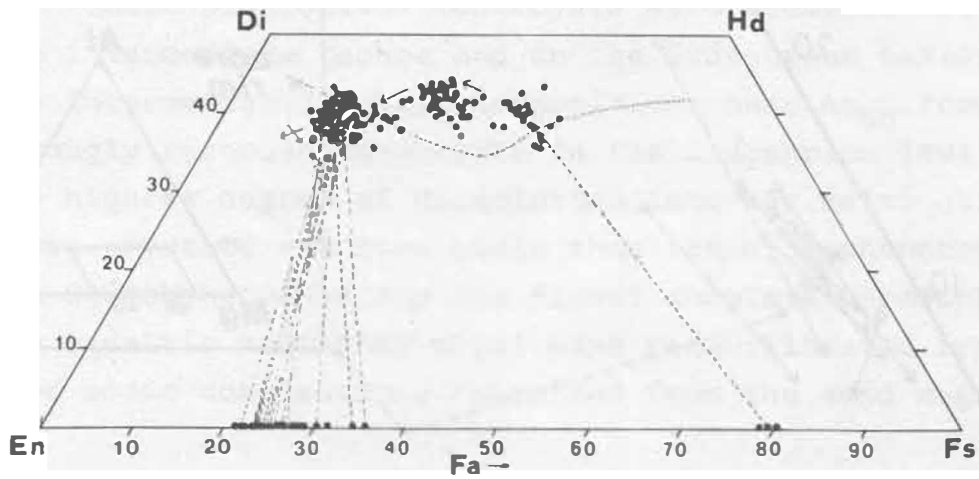


Fig. 8a..
Total clinopyroxene analyses plotted in the En-Fs-Di-Hd quadrilateral, with main zoning directions marked by arrows. Tie-lines connect coexisting olivine and clinopyroxene. Skaergaard trend is drawn for comparison.

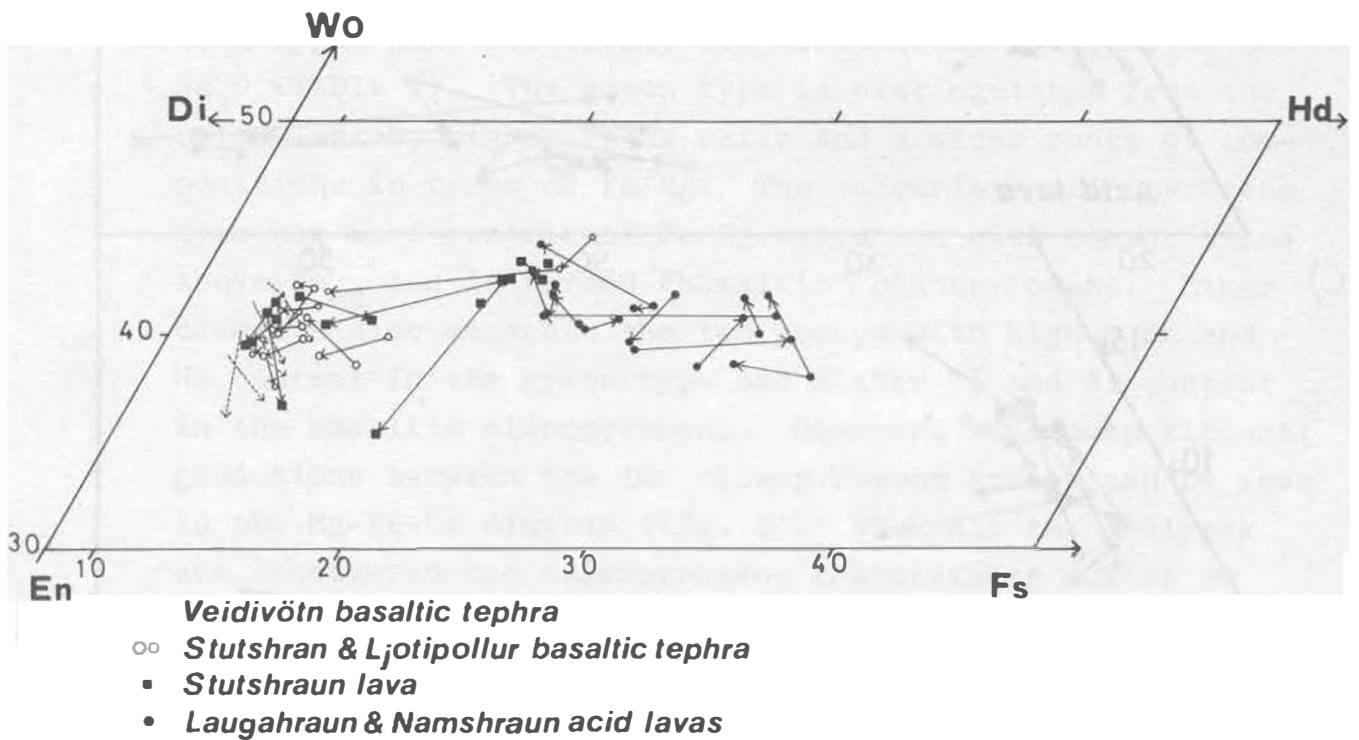


Fig. 8b.
Clinopyroxene zoning in the various rock-types plotted in the En-Fs-Di-Hd quadrilateral.

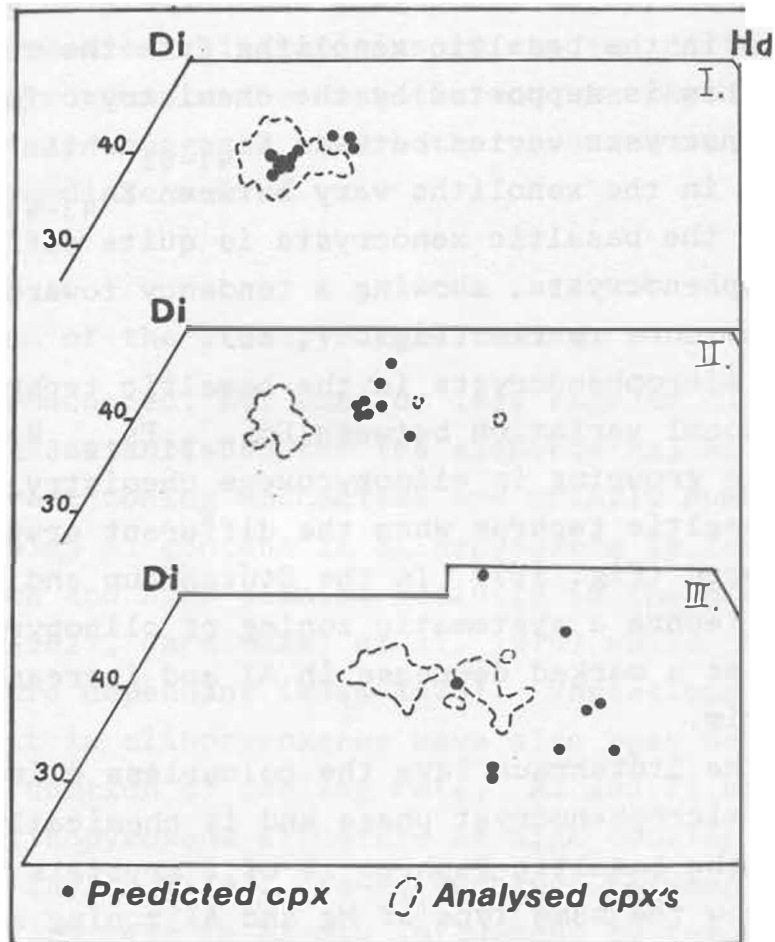


Fig. 8c.
Comparison between analysed clinopyroxene (shown by general areas) and calculated compositions by the method of Nielsen & Drake (1979):
I. Stutshraun tephra. II. Namshraun tephra. III. Acid lava matrix.

tent from core to margin. The most Mg rich margins are also the most Ca rich. No Al zoning is recorded.

The colourless clinopyroxene grains in the acid lavas were interpreted as xenocrysts and correlated with clinopyroxenes in the basaltic xenoliths from the textural relations. This is supported by the chemistry: The En content of the xenocrysts varies between En_{41-51} while the clinopyroxenes in the xenoliths vary between En_{43-49} . Mineral zoning of the basaltic xenocrysts is quite different from the microphenocrysts, showing a tendency toward decreasing Mg/Fe from core to rim (Figs. 7, 8b).

The microphenocrysts in the basaltic tephra have a compositional variation between $En_{50-31}Fs_{19-6}Wo_{40-27}$. No systematic grouping in clinopyroxene chemistry can be seen in the basaltic tephra when the different eruption sites are compared (Fig. 10). In the Stútshraun and Ljótípollur basaltic tephra a systematic zoning of clinopyroxene is observed as a marked decrease in Al and increase in Mg from core to rim.

In the Stútshraun lava the colourless clinopyroxene is a common microphenocryst phase and is chemically similar to those in the basaltic tephra. 4 of 5 crystals examined for zoning show the same type of Mg and Al zoning as described for the microphenocrysts in the Stútshraun and Ljótípollur tephra.

Green euhedral xenocrysts in this lava are chemically similar to the microphenocrysts (green, Fe rich type) in the rhyolitic lavas. One of these xenocrysts is strongly zoned with an outer rim of similar basaltic composition as the microphenocrysts in the lava.

The dominant clinopyroxene in the intermediate tephra is colourless with the same chemistry and appearance as in the basaltic tephra. The clinopyroxene zoning is, however, different from the systematic zoning recorded in the Stútshraun and Ljótípollur basaltic tephra showing slight Mg decrease and Al increase rimwards. This zoning can better be compared with the zoning described for the basaltic

clinopyroxene xenocrysts in the acid lavas.

The green clinopyroxene is less common. The chemistry is similar to the microphenocrysts in the acid lavas, but zoning is not recorded.

The chemical similarities to the two different groups of clinopyroxene in the basaltic and the rhyolitic melts respectively suggests that both types are xenocrysts in the intermediate melts.

Discussion of the clinopyroxene zoning

A pronounced, but more or less regular clinopyroxene zoning was established for the elements Mg, Al, Fe and Ca, and relevant zoning mechanisms are briefly summarized below: High Al content in clinopyroxene is favoured by low silica and high alumina activity in the host magma (Le Bas 1962), Carmichael et al. 1974) while the Al^{VI}/Al^{IV} is pressure dependant (Wass 1979). Variations in Al and Ti content in clinopyroxenes have also been demonstrated to be a function of cooling rate; Al and Ti may be trapped in the clinopyroxene structure at high cooling rates (Coish & Taylor 1979). Fe-Mg exchange between clinopyroxene and melt is hardly influenced by temperature and is controlled by the chemistry of the magma (Duke 1976). Increasing Fe/Mg ratio in clinopyroxenes during differentiation in comagmatic melts is the normal evolution trend caused by the Fe/Mg increase of the melt. The inverse clinopyroxene zoning has been explained by increasing f_{O_2} resulting in change of magma composition due to precipitation of iron oxides (or due to reaction relationships between ortho- and clinopyroxene) (Hewins 1974).

In the present study the influence of magma chemistry is important. Different zoning patterns were found in the green and colourless (basaltic) clinopyroxene types. The same clinopyroxene type also showed zoning patterns in the different melt environments.

In the acid lavas the contrasted zoning patterns of the microphenocrysts and the xenocrysts are compared in the Mg-Fe-Al diagram (Fig. 7), and are explained by mixing. The increasing Mg/Fe towards the rims in the microphenocrysts (green cpx) (Fig. 7b) can be explained by contamination of the acid melt with the basaltic melt as evidenced by the numerous xenoliths. Local Mg/Fe enrichments in the acid melt could also have been caused by the simultaneous crystallization of magnetite, but clinopyroxene domains in contact with magnetite do not show special Mg/Fe enrichment. The opposite zoning pattern found in the basaltic xenocrysts in the acid lavas supports the mixing influence on clinopyroxene chemistry. The same zoning is recorded by the basaltic clinopyroxene xenocrysts in the intermediate tephra (Fig. 7c), but not in the basalts (Fig. 7a). On the other hand the zoning of the basaltic xenocrysts (Fe/Mg increase rimwards) is the normal zoning to be expected during fractional crystallization and may therefore even have formed before the magma mixing.

In the basaltic melts from Stútshraun and Ljótípollur eruption sites the systematic zoning with Mg increase and Al decrease from core to rim cannot be unambiguously explained. The Al pattern might be caused by cooling-rate effects but might also reflect Al decrease in the magma due to plagioclase crystallization. Increasing f_{O_2} would favour Mg enrichment and cause this reverse zoning, as would also a more complex basaltic mixing history with new batches of less differentiated magma. The plagioclase zoning excludes the latter.

The green clinopyroxene xenocrysts in basaltic melts most clearly demonstrate the influence of magma chemistry upon clinopyroxene composition. Both in the Ljótípollur tephra and in the Stútshraun lava these xenocrysts are zoned with increasing Mg rimwards, and the composition of the outer rim is similar to the basaltic microphenocrysts in the tephra and lava, while the core compositions are similar to microphenocrysts in the rhyolitic lavas. This strongly suggests that the Fe rich xenocrysts formed in the

rhyolitic magma and adjusted towards basaltic chemistry after entering into the basaltic melt. The zoning patterns either indicate that the outer margin was modified chemically by diffusion from the melt or that the crystals acted as nucleation sites for further clinopyroxene crystallization in the basaltic melt. Abrupt changes only in the outer margin favour the latter mechanism in the Stútshraun lava. The xenocryst studied in the Ljótípollur tephra showed gradual zoning. In this case either the adjacent melt composition must have changed gradually or the original composition was modified by diffusion from the basaltic melt.

Olivine variation

The total variation in Fo content in the basaltic tephra is between Fo₇₅₋₇₉ without clear zoning of crystals (Table 4). The olivines in the Stútshraun lava are more iron rich with a total variation Fo₆₄₋₇₀ and are zoned with a Fo decrease of four units from core to rim (Table 4). MnO shows a systematic increase from core to rim in the olivine in the Stútshraun lava, reflecting the positive correlation of MnO with FeO.

Only one olivine phenocryst was analyzed in the rhyolitic lavas (Námshraun lava). It is zoned from Fo_{19.9} in the core to Fo_{21.6} in the rim, and it also differs from the basaltic olivines in having distinctly higher MnO content (~2% MnO). Olivine also occurs as basaltic xenocrysts in the acid lavas and in intermediate tephra where it covers a greater composition range than recorded for the microphenocrysts in basaltic tephra. The xenocrysts in the acid lavas show a clear decrease in Fo content and increase of Mn rimwards. Zoning is also pronounced in olivine xenocrysts in the intermediate tephra, but less systematic.

The opposite zoning trends for pheno- and xenocrysts in the acid lavas are in accordance with the zoning re-

corded for clinopyroxene in the same lavas. This shows that olivines also have been influenced by the mixing of the two magmas. The slightly more Fe rich olivines in the Stútshraun lava compared to the basaltic tephra, and the stronger zoning, is in accordance with the other findings: This lava has a slightly more differentiated chemistry and higher content of "acid" xenocrysts than the basaltic tephra, reflecting mixing with an acid contaminant. The zoning patterns demonstrate that crystallization continued after the mixing event in this lava.

Mineral - melt equilibria and sources of phenocrysts

The high abundance of xenocrysts in the melts, together with the contrasted zoning behaviour of phenocrysts and xenocrysts in the same rock, supports the interpretation of magma mixing. But even in the end member magmas equilibrium between phenocrysts and melt is not obvious, due to the mineral zoning. From textural and mineral-chemical criteria these magmas are interpreted as the sources of the numerous xenocrysts. But the complex mixing history makes it difficult to decide if the minerals are in equilibrium with any of the present glass compositions.

The range of mineral chemistry for clinopyroxene, plagioclase, and olivine is compared with the total range of glass compositions in Fig. 11. While intermediate melts are abundant, associated intermediate mineral compositions are very scarce. This may be a result of the relative time sequence of eruption since the mixed intermediate tephra erupted very early in the sequence, probably immediately after the mixing. In contrast, in the later-erupted lavas phenocrysts and to some extent xenocrysts (especially in the Stútshraun lava) had time to reequilibrate (partly).

The melts present before the mixing are most closely represented by the rhyolitic parts of the acid lavas (and tephra), and the basaltic tephra. Before the magmas were

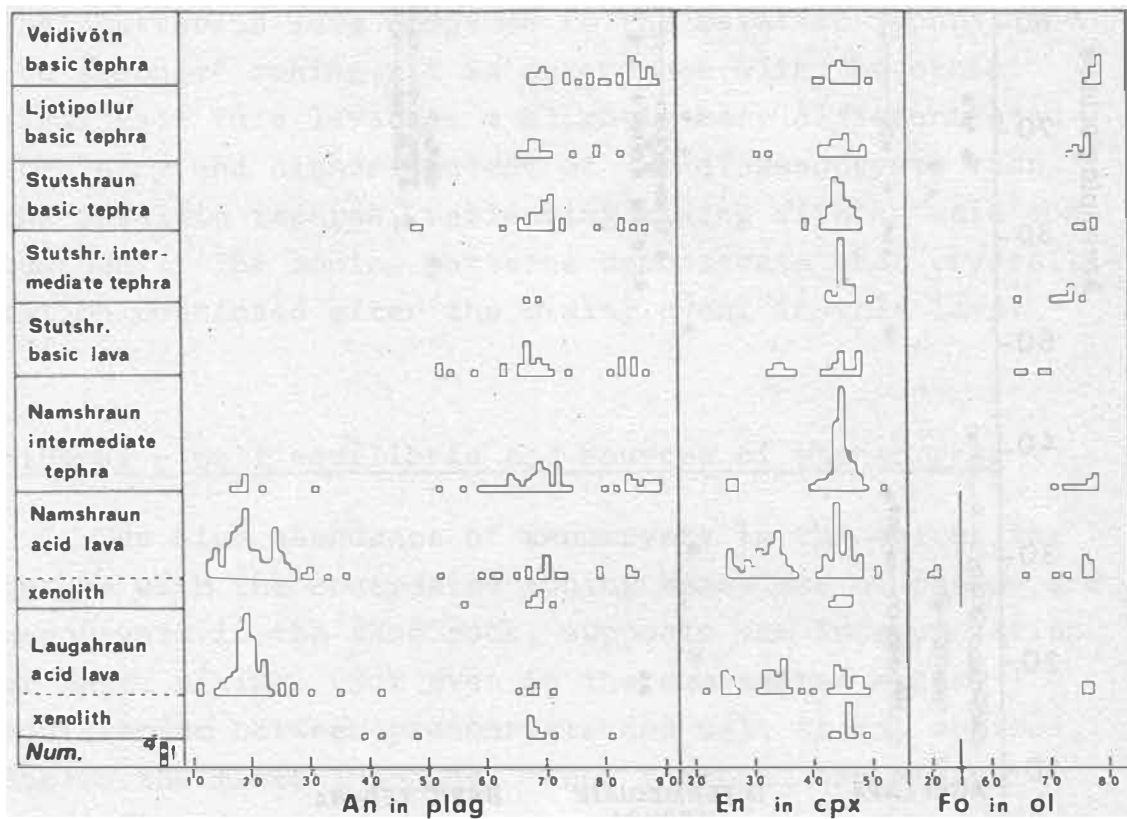


Fig. 10. Comparison of mineral chemistry for the main glass types at the various eruption sites. The samples are grouped from north to south along the Veidivötn line. The mineralogy is for simplicity expressed by the contents of the components En, An and Fo in clinopyroxene, plagioclase and olivine.

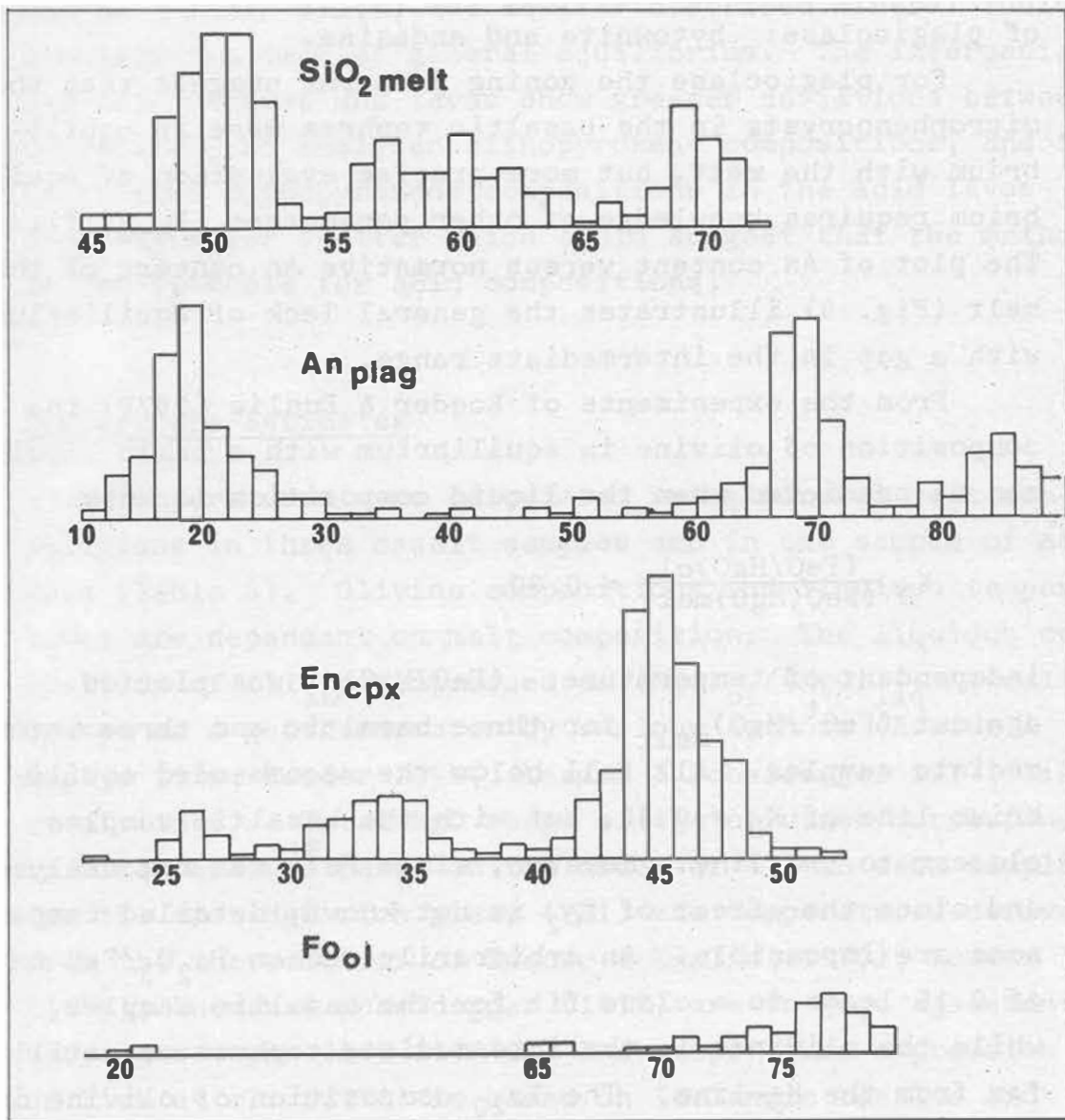


Fig. 11.
Comparisons of mineral chemistry and glass chemistry including all the analyses in the present study.

mixed, the rhyolitic magma was crystallizing oligoclase, olivine (Fo_{20}), ferroaugite and magnetite. The basaltic magma contained olivine (Fo_{75}), augite and two generations of plagioclase: bytownite and andesine.

For plagioclase the zoning patterns suggest that the microphenocrysts in the basaltic tephras were in equilibrium with the melt, but more precise evaluation of equilibrium requires knowledge of other parameters ($P_{\text{H}_2\text{O}}$, T). The plot of An content versus normative An content of the melt (Fig. 9) illustrates the general lack of equilibrium with a gap in the intermediate range.

From the experiments of Roeder & Emslie (1970) the composition of olivine in equilibrium with a basic liquid can be predicted when the liquid composition is known:

$$K_D \frac{(\text{FeO}/\text{MgO})_{\text{ol}}}{(\text{FeO}/\text{MgO})_{\text{melt}}} = 0.30$$

independent of temperature. $(\text{FeO}/\text{MgO})_{\text{ol}}$ was plotted against $(\text{FeO}^{\text{t}}/\text{MgO})_{\text{melt}}$ for three basaltic and three intermediate samples. All fall below the recommended equilibrium line of $K_D = 0.30$, but with the basaltic samples closest to the line. However, since Fe^{3+} was not analysed, and since the effect of f_{O_2} is not known, detailed comparisons are impossible. An arbitrarily chosen $\text{Fe}_2\text{O}_3/\text{FeO}$ ratio of 0.15 leads to a close fit for the basaltic samples, while the olivines in the intermediate tephras are still far from the K_D -line. The Fo_{20} composition of olivine in the acid lava would also plot on the extension of the line, but the diagram is not calibrated for acid compositions.

Clinopyroxene composition can be predicted from melt composition from the set of equations formulated by Nielsen & Drake (1979), based on thermodynamic mixing models for clinopyroxene melt. Using their iterative procedure a set of clinopyroxene compositions and temperatures can be calculated from given melt compositions. For the basaltic tephras the calculated clinopyroxene compositions are in excellent agreement with the mean values for the

analysed clinopyroxenes, and indicate that the clinopyroxenes in the basaltic tephras formed in those melts. But on a finer scale, the earlier described mineral zoning demonstrates lack of general equilibrium. The intermediate and acid tephras and lavas show greater deviations between calculated and analysed clinopyroxene compositions, and the calculated clinopyroxene compositions in the acid lavas show a greater scatter which could suggest that the method is not suitable for acid compositions.

Temperature estimates

Temperatures were calculated using mineral melt compositions in three basalt samples and in one sample of acid lava (Table 5). Olivine compositions and liquidus temperatures are dependant on melt composition. The liquidus composition of olivine expressed as $(\text{MgO})_{\text{ol}}/(\text{MgO})_{\text{liq}}$ is calibrated as a geothermometer by various authors (Roeder & Emslie 1970, Roeder 1974, Leeman & Scheidegger 1977, Fisk et al. 1978). Total MgO range of the olivines corresponds to a temperature range on the order of 5°C in each sample. For the most MgO rich glass (VE1) the temperatures derived from the thermometers of Roeder & Emslie (1970), Roeder (1974), Leeman & Scheidegger (1977) are in good agreement, varying between 1166-1177°C. The temperature expression of Fisk et al. (1978) is based on Icelandic basalts and gives significantly lower values (Table 5).

Tholeiitic basalts from Iceland and the Reykjanes Ridge have olivine-liquid temperatures in the range 1150-1240°C (Fisk et al. 1978). Increase of the FeO/MgO ratio and of SiO₂ in the melt may however cause a lowering of the liquidus temperature. In the present study the Veidivötn sample shows the closest fit to the liquidus temperature-composition relations of Fisk et al. (1980) falling precisely on the liquidus line for the Reykjanes Ridge basalts. Using the arguments of Fisk et al. (1978,

1980) the higher temperatures derived for the Stútshraun tephra may be related to the lower silica content in this glass (but the FeO/MgO ratio of this sample is slightly higher than in the Veidivötn sample). The Ljótípollur tephra which gives the lowest T-values is also more differentiated with respect to SiO₂ and the FeO/MgO-ratio.

The clinopyroxene-melt iteration procedure of Nielsen & Drake (1979) gives temperatures in the range 1143-1149°C for the basaltic tephra. These are distinctly lower than the olivine-melt temperatures, and may reflect the later crystallization of clinopyroxene, and that clinopyroxene and olivine have not reequilibrated to the same extent.

For the acid compositions mafic mineral-melt thermometers are not available. Temperatures versus P_{H₂O}'s are, however, given in Table 5c using the Kudo & Weill (1970) thermometer for coexisting plagioclase-liquid. These indicate that the silicic melt was far above the minimum melting temperature for the granitic system for reasonable P_{H₂O}'s.

CONCLUSIONS AND IMPLICATIONS

Veidivötn eruption compared with regional petrology

The chemical suite studied here is interpreted as a product of mixing between basaltic and acid end member magmas. While the basalt is tholeiitic, the rhyolite is more alkaline and the intermediate mixing products are transitional. The resulting rock suite is characterized by a steep trend in the alkali-silica diagram, intersecting both alkaline and sub-alkaline differentiation trends from Iceland (Fig. 5). However, the four craters studied only constitute a minor part of the Veidivötn fissure eruption. According to Jakobsson (1979) the Veidi-

vötn fissure swarm is a closed volcanic system which has produced mainly basalts, and a central volcano with silicic activity is not developed. The southernmost part of the eruption is therefore exceptional for its large amounts of silicic rocks. Also, the xenocryst content increases and the compositional range of phenocrysts becomes more complex at the southern part of the Veidivötn fissure. This means that there is a regional control on magma compositions.

The differences in alkalinity between the acid and basaltic end members are also in accordance with regional petrology (Jakobsson 1972). The Veidivötn fissure intersects an important petrological boundary in southeast Iceland where the eastern rift zone terminates in the Sudurland zone of transgressive volcanism (Oskarsson et al. 1979). While the rift zone volcanism is tholeiitic, the transgressive volcanism is more alkaline and is chemically more heterogeneous. Thus, in the Veidivötn eruption, melts were formed in the two petrological provinces, were mixed shortly before the eruption and erupted simultaneously as a sequence of different melt compositions. Silicic melts were only erupted inside or close to the Torfajökull silicic centre while the basaltic melts erupted to the north and the intermediate and most heterogeneous melts erupted just at the contact between the different petrological areas.

End member magmas

The most homogeneous and K poor tephra from the basaltic craters satisfy the criteria proposed by Shido & Miyoshiro (1971) for abyssal tholeiites, except for the high FeO/MgO ratio which prevents even the most basic glasses from being regarded as primary compositions (Maalöe 1979). This feature characterizes most postglacial basalts in the area. According to Jakobsson (1979) approximately half of the extruded basalt lavas of the eastern volcanic zone have either lost or accumulated microphenocrysts, and

in the Veidivötn volcanic system plagioclase porphyric lavas are common through time. All the melts studied must be considered as chemically modified. Even the most basaltic melts studied show textural evidence of a complex evolution. Slightly oscillatory zoning (recorded optically) in the Ca-richer cores of bytownite phenocrysts might even reflect crystal sinking within a basaltic magma chamber before the calcium poorer rims and the microphenocrysts formed. The cores may have formed from the more primitive magma. The high FeO/MgO ratio of the melts, however, indicates either that mafic phases were also fractionating early or that the magma was modified by mixing processes (or both). Various relations suggest that the mafic microphenocrysts found in the melts did not crystallize from a primary magma composition. These include relatively high FeO/MgO ratio in olivines and clinopyroxenes and the appearance of these phases in glomerocrysts with the second stage of plagioclase crystals. On the other hand the crystallization of the few percent (<5) of mafic microphenocrysts observed in the tephra has caused only a slight increase of the FeO/MgO ratio of the melt. The melts have therefore been modified before the microphenocrysts formed.

The acid magma originated within the Torfajökull silicic centre. Due to the lack of appropriate basaltic source compositions in the eruption products the rhyolites are interpreted as a result of shallow melting of the silicic crust. From the regional distribution of the different eruption products it is also most likely that a shallow acid magma chamber existed before the mixing with the tholeiitic magma. It was argued earlier that even the most silicic melts of the eruption sequence had been modified chemically by mixing so that the original acid magma probably is not represented in the lavas and tephra studied here.

Magma mixing and eruption

Since both the acid and the basaltic magma had formed microphenocrysts before the mixing, there must have been at least two magma chambers or reservoirs present. The evolved basaltic magma was stored long enough to form the abundant olivine-plagioclase-clinopyroxene glomerocrysts and for partial reequilibration of the calcium rich plagioclase phenocrysts. The acid magma also existed in a magma chamber and crystals of plagioclase-olivine-clinopyroxene-magnetite had formed before the mixing, but these crystals continued to grow during the mixing as well.

At some time before eruption the basaltic magma with its reequilibrated microphenocrysts was remobilized, and part of it intruded into the rhyolitic magma chamber. This resulted in rapid mixing of melts to form the intermediate Námshraun tephra, and of further contamination of larger volumes of acid melts. The crystals found in the mixed tephra are mostly inherited from the acid and basaltic magmas. This stage of magma mixing therefore occurred shortly before the Námshraun tephra was erupted. From the discussion of the positions of the mixed tephra layers in the Námshraun and Stútshraun profiles it is possible that the first phreatomagmatic, explosive phase in the Stúts-hraun crater, that marked the start of eruption, may also have been simultaneous with the mobilization of the basalt and the start of magma mixing.

The bulk of acid magma erupted later, as lavas with relicts of chilled basaltic melt fragments (xenoliths) and partly resolved glomerocrysts (xenocrysts). In this contaminated silicic magma chamber the minerals had time to reequilibrate in part and crystallization continued during mixing. The effects of contamination/mixing with the hotter, basaltic melt were partial resorption of sodic plagioclase with replacement by Ca richer margins, and rimwards Mg-increase in mafic phases.

The Stútshraun basaltic lava is similarly derived by mixing of minor amounts of silicic melts and phenocrysts

into larger volumes of basalt. Here the basaltic phenocrysts equilibrated rimwards towards a more differentiated chemistry while acid xenocrysts were either partly resorbed or oppositely zoned.

Magma mixing and formation of intermediate magmas

Magma mixing is a process which is usually associated with continental crust and compressional tectonics, while oceanic crust and extensional tectonics results only in a small rhyolitic component and little mixing (Eichelberger 1974). In contrast, Oskarsson et al. (1979) consider magma mixing to be an important part of rift zone petrogenesis. The Veidivötn eruption studied gives an example of magma mixing and of contemporaneous eruption of unrelated rhyolitic and basaltic magmas. But the main implications of the present study concern the role of magma mixing for the formation of intermediate melts.

Acid and basaltic magmas have erupted simultaneously in many cases in Iceland. In some places the basaltic magma has intruded into a shallow rhyolitic magma chamber shortly before the eruption (Walker & Skelhorn 1966, Sparks et al. 1977, Sigurdsson & Sparks 1978, Sigvaldason 1979). The intrusion of a basaltic magma into a colder acid magma leads to two competing processes: Mixing with formation of magma of intermediate compositions (if completed) and a triggering of an eruption due to superheating and devolatilization of the acid magma (Sigurdsson & Sparks 1973). Due to rapid quenching of the basaltic melt in contact with dacite during ascent of the Askja magma intermediate melts did not have time to form (Sigvaldason 1979). In this case the result is a heterogeneous mixture of dacite and basaltic xenoliths. But, according to Sigurdsson & Sparks (1981) the mixing resulted in chemical hybridization of the rhyolite as well.

Such mixtures are typical also in the Laugahraun and Námshraun silicic lavas described in this study but here

the mixing went even further with formation of intermediate melts and slightly chemically modified silicic melts. Homogeneous glasses were formed (microscale) both in the tephra and in the lavas. This, together with the close association of these melts in space and time, and the mineral criteria, demonstrate that both the acid and the basic components existed as melts simultaneously. It was concluded that the basaltic melt intruded into the acid melt. The apparently "solid" character of the xenoliths representing the basic contaminant in the silicic lavas is due to early chilling and quenching of the basaltic melt inclusions in the colder silicic magma chamber. In marginal parts of the silicic magma chamber below the Námshraun eruption site, rapid mixing took place producing intermediate melts. This process apparently continued on the way up, and the slightly differently mixed melts froze into streaked pumice on reaching the air.

ACKNOWLEDGEMENTS

This work is part of a project at the Nordic Volcanological Institute, Reykjavik and was proposed by Guðrún Larsen and Karl Grönvold for my one year fellowship there, supported by the Nordic Council. G. Larsen selected the tephra sampling locations and her unpublished tephrastratigraphy of the Landmannalaugar-Veidivötn area is the basis for this study. G. Larsen and Dr. Grönvold are acknowledged for field guidance and for criticism of the first report, and I would also like to thank the other colleagues at the institute for various practical advice.

REFERENCES

- Carmichael, I.S.E. 1964: The petrology of Thingmuli, a Tertiary volcano in Eastern Iceland. J. Petrol. 5, 435-460.
- Carmichael, I.S.E., Turner, F.J. & Verhoogen, J. 1974: Igneous Petrology. McGraw-Hill Book Company, 739 pp.
- Coish, R.A. & Taylor, L.A. 1979: The effect of cooling rate on texture and pyroxene chemistry in DSDP LEG 34 basalt: A microprobe study. Earth Planet. Sci. Lett. 42, 389-398.
- Duke, J.M. 1976: Distribution of the period four transition elements among olivine, calcic clinopyroxene and mafic silicate liquid: experimental results. J. Petrol. 17, 499-521.
- Eichelberger, J.C. 1974: Magma contamination within the volcanic pile: origin of andesite and dacite. Geology 2, 29-33
- Fisk, M.R., Schilling, J.-G. & Sigurdsson, H. 1978: Olivine geothermometry of Reykjanes Ridge and Iceland tholeiites. EOS 59, 410.
- Fisk, M.R., Schilling, J.-G. & Sigurdsson, H. 1980: An experimental investigation of Iceland and Reykjanes Ridge tholeiites: I. Phase relations. Contrib. Mineral. Petrol. 74, 361-374.
- Grönvold, K. & Mäkipää, H. 1978: Chemical composition of Krafla lavas 1975-1977. Nordic Volc. Inst. 7816, 49 pp.
- Hewins, R.H. 1974: Pyroxene crystallization trends and contrasting augite zoning in the Sudbury nickel eruptive. Am. Mineral. 59, 120-126.

- Irvine, T.N. & Baragar, W.R.A. 1971: A guide to chemical classification of the common volcanic rocks. Can. J. Earth Sci. 8, 523-548.
- Jakobsson, S.P. 1972: Chemistry and distribution pattern of recent basaltic rocks in Iceland. Lithos 5, 365-386.
- Jakobsson, S.P. 1979: Petrology of recent basalts of the eastern volcanic zone, Iceland. Acta Naturalia Islandica 26, 103 pp.
- Kjartansson, G. 1962: Geological map of Iceland, Sheet 6, South-Central Iceland, 1:250.000. Iceland Geodetic Survey 1977.
- Kudo, A.M. & Weill, D.F. 1970: An igneous plagioclase thermometer. Contrib. Mineral. Petrol. 25, 52-65.
- Larsen, G. 1978: Gjóskulög í nágrenni Kötlu. (Tephra layers in the vicinity of Katla). Unpubl. B.Sc.Hon. thesis, 66 pp. University of Iceland.
- Larsen, G. 1980: Explosive basaltic fissure eruptions on the Torfajökull-Veidivötn fissure swarm in south Iceland. Abstract. In: Tephra Studies as a Tool in quaternary Research. A NATO Advance Study Institute Iceland 1980.
- Le Bas, M.J. 1962: The role of aluminium in igneous clinopyroxenes with relations to their parentage. Am. J. Sci. 260, 261-288.
- Leeman, W.P. & Scheidegger, K.F. 1977: Olivine/liquid distribution coefficients and a test for crystal-liquid equilibrium. Earth Planet. Sci. Lett. 35, 247-257.
- Maalöe, S. 1979: Compositional range of primary tholeiitic magmas evaluated from major-element trends. Lithos 12, 59-72.

- Miyashiro, A. 1978: Nature of alkalic volcanic rock series. Contrib. Mineral. Petrol. 66, 91-104.
- Nielsen, R.L. & Drake, M.J. 1979: Pyroxene-melt equilibria. Geochim. Cosmochim. Acta 43, 1259-1272.
- O'Nions, R.K. & Grönvold, K. 1973: Petrogenetic relationships of acid and basic rocks in Iceland: Sr-isotopes and rare-earth elements in late and postglacial volcanics. Earth Planet. Sci. Lett. 19, 397-409.
- Oskarsson, N., Sigvaldason, G. & Steinthorsson, S. 1979: A dynamic model of rift zone petrogenesis and the regional petrology of Iceland. Nordic Volc. Inst. 7905 & Sci. Inst. 7916, 104 pp.
- Roeder, P.L. 1974: Activity of iron and olivine solubility in basaltic liquids. Earth Planet. Sci. Lett. 24, 397-410.
- Roeder, P.L. & Emslie, R.F. 1970: Olivine-liquid equilibrium. Contrib. Mineral. Petrol. 29, 275-289.
- Shido, F. & Miyashiro, A. 1971: Crystallization of abyssal tholeiites. Contrib. Mineral. Petrol. 31, 251-266.
- Sigurdsson, H. 1970: The petrology and chemistry of the Setberg volcanic region and of the intermediate and acid rocks of Iceland. Unpubl. Ph.D. thesis. Univ. of Durham, 308 pp.
- Sigurdsson, H. 1971: Feldspar relations in a composite magma. Lithos 4, 231-238.
- Sigurdsson, H. & Sparks, R.S.J. 1978: Rifting episode in North Iceland in 1874-1875 and the eruption of Askja and Sveinagja. Bull. Volcanol. 41, 149-167.
- Sigurdsson, H. & Sparks, R.S.J. 1981: Petrology of rhyolitic and mixed magma ejecta from the 1875 eruption of Askja, Iceland. J. Petrol. 22, 41-84.

- Sigvaldason, G.E. 1979: Rifting, magmatic activity and interaction between acid and basic liquids. The 1875 Askja eruption in Iceland. Nordic Volc. Inst. 7903, 54 pp.
- Sparks, R.S.J., Sigurdsson, H. & Wilson, L. 1977: Magma mixing: A mechanism for triggering acid explosive eruptions. Nature 267, 315-318.
- Sæmundsson, K. 1972: Jarðfræðiglefsur um Torfajökulsvæðid. Náttúrufræðingurinn 42, 81-99.
- Walker, G.P.L. & Skelhorn, R.R. 1966: Some associations of acid and basic igneous rocks. Earth Sci. Rev. 2, 93-104.
- Wass, S.Y. 1979: Multiple origin of clinopyroxenes in alkali basaltic rocks. Lithos 12, 115-132.
- Wetzel, R., Wenk, E., Stern, W. & Schwander, H. 1978: Beiträge zur Petrographie Islands. Vulkaninstitut I. Friedlaender, Zürich 10, 128 pp.

	SiO ₂	TiO ₂	Al ₂ O ₃	FeO ^t	MnO	MgO	CaO	Na ₂ O	K ₂ O	P ₂ O ₅	
<u>Namshraun tephra.</u>											
N-5	57.91	1.56	14.78	9.89	0.18	2.59	6.09	4.12	1.82	0.15	99.09
N-4	56.92	1.37	14.81	9.68	0.16	2.54	6.15	4.97	1.83	0.15	98.58
N-3	58.76	1.40	14.92	9.37	0.19	2.41	6.12	4.31	1.94	0.17	99.59
N-2	64.25	0.55	14.81	5.42	0.13	0.99	2.47	5.49	3.26	0.09	97.46
N-2	60.77	0.89	15.12	6.80	0.12	1.67	4.05	5.34	2.70	0.14	97.60
N-1	60.98	1.01	15.15	8.03	0.14	1.80	4.75	4.40	2.57	0.13	98.96
N-1	69.54	0.38	14.41	3.52	0.14	0.25	1.12	4.72	4.35	0.07	98.50
N1-A1	60.79	0.97	15.25	7.47	0.13	1.75	5.01	4.63	2.58	0.10	98.68
N1-A2	62.15	0.89	15.12	6.51	0.10	1.43	4.23	4.34	2.79	0.11	97.67
<u>Stutshraun tephra.</u>											
S-8	49.32	2.12	13.54	13.46	0.22	6.43	10.97	2.51	0.27	0.22	99.06
S-7	51.06	1.80	13.27	13.27	0.20	5.61	11.13	2.12	0.36	0.16	98.98
S-6	49.55	2.00	13.57	13.44	0.25	6.14	10.89	2.57	0.27	0.18	98.86
S5b(1)	57.28	1.13	14.62	8.91	0.14	2.89	6.71	4.14	1.88	0.14	97.84
S5b(2)	58.51	1.28	15.32	8.59	0.14	2.34	5.47	4.47	2.12	0.15	98.39
S5b(3)	60.51	1.20	14.79	8.20	0.14	2.11	5.29	4.73	2.34	0.13	99.44
S5a(1)	49.54	1.83	13.96	13.51	0.19	5.88	11.09	2.66	0.31	0.20	99.17
S5a(1)	58.00	1.24	15.83	8.82	0.18	2.53	6.11	3.91	1.92	0.15	98.69
S5a(2)	69.57	0.27	14.59	2.88	0.09	0.21	1.23	5.17	4.38	0.09	98.48
S-4	49.76	1.93	13.68	12.65	0.26	5.40	10.34	2.96	0.61	0.20	97.79
S-3	51.60	1.80	14.17	11.95	0.19	5.60	10.23	2.76	0.60	0.18	99.08
SÖ-1	52.15	1.72	14.68	12.12	0.25	5.32	10.00	2.93	0.57	0.19	99.93
SÖ-2	51.75	1.79	14.38	12.26	0.24	5.20	10.07	3.12	0.61	0.19	99.61
S-2	50.67	1.74	13.68	12.22	0.26	5.09	10.03	3.11	0.67	0.18	97.65
S-1	50.46	1.86	14.04	12.61	0.20	6.01	10.48	2.74	0.47	0.20	99.07
<u>Ljotipollur tephra.</u>											
Lj-3	49.05	2.33	13.73	12.78	0.23	6.11	10.98	2.92	0.27	0.18	98.58
Lj-2	51.49	1.96	14.10	13.02	0.22	5.46	10.03	2.63	0.59	0.21	99.71
Lj-1	50.56	2.68	13.56	12.43	0.25	5.59	9.97	2.79	0.47	0.17	98.47
<u>Veiðivötn tephra.</u>											
VE-1	49.66	1.86	13.43	12.68	0.22	6.33	11.71	2.45	0.26	0.18	98.78

Table 1a. Microprobe analyses of matrix-glass of tephra. The sample numbers represent mean values of point analyses for basaltic tephra and mean values of microscan over domains about a tenth of a mm size for intermediate and acid tephra. The mean values represent homogeneous domains of large pumice clasts or similar compositions of different grains from bulk samples representing a tephra layer.

	<u>SiO₂</u>	<u>TiO₂</u>	<u>Al₂O₃</u>	<u>FeO^t</u>	<u>MnO</u>	<u>MgO</u>	CaO	Na ₂ O	<u>K₂O</u>	<u>P₂O₅</u>	
<u>Laugahraun lava.</u>											
L-1	70.94	0.38	14.44	3.51	0.12	0.24	1.09	5.58	4.25	0.05	100.60
L-2	69.57	0.34	14.19	3.03	0.13	0.18	1.20	5.53	4.37	0.07	98.61
L-5	70.53	0.29	13.87	2.54	0.10	0.27	0.64	5.70	4.59	0.07	98.60
<u>Namshraun lava.</u>											
NH-2	69.19	0.49	15.03	3.49	0.09	0.39	1.72	5.58	3.96	0.09	100.03
NH-3	66.13	0.89	14.25	5.76	0.11	0.80	2.52	5.26	3.82	0.17	99.71
NH-6	70.23	0.35	13.68	2.76	0.08	0.15	0.58	5.77	4.89	0.04	98.50
NH-9	70.53	0.30	13.34	3.16	0.09	0.18	0.87	5.15	4.62	0.05	98.29
NH-10	71.51	0.36	14.02	2.35	0.05	0.26	0.58	5.31	5.38	0.05	99.87

Table 1b. Microprobe analyses of glassy lava matrix, representing mean values of microscan areas (as described for intermediate and acid tephra) of a thin section.

Lavas.	<u>SiO₂</u>	<u>TiO₂</u>	<u>Al₂O₃</u>	<u>FeO</u>	<u>MnO</u>	<u>MgO</u>	<u>CaO</u>	<u>Na₂O</u>	<u>K₂O</u>	<u>P₂O₅</u>	
SH2a	53.35	1.54	14.49	10.25	0.22	5.14	9.97	2.87	0.95	0.13	98.91
SH2b	53.78	1.47	14.31	10.11	0.21	5.12	9.82	2.83	0.97	0.14	98.76
SH9	54.72	1.25	13.99	9.50	0.18	4.93	9.52	2.81	1.04	0.13	98.07
L6	71.77	0.28	13.66	2.64	0.08	0.21	1.00	4.90	4.75	0.05	99.34
NH1a	67.55	0.54	14.48	4.48	0.11	0.86	2.64	5.11	3.91	0.11	99.79
Xenoliths.											
NH1	52.07	1.64	13.68	11.27	0.22	5.85	10.86	2.78	0.64	0.16	99.16
NH8	57.45	1.20	14.27	8.67	0.15	3.76	7.47	3.89	2.01	0.11	98.98
L4	58.08	1.15	14.50	9.44	0.15	3.70	7.36	3.98	1.84	0.14	100.34

Table 2 . Microprobe analyses of fused samples from Stutshraun lava, Laugahraun lava and of xenoliths from the Namshraun and Laugahraun lavas. NH1 is the largest of the xenoliths studied, and the acid glass NH1a is picked out less than 1 cm from the xenolith contact. SH2a is slightly more crystalline than SH2b.

CLINOPYROXENE.

		SiO ₂	TiO ₂	Al ₂ O ₃	FeO	MnO	MgO	CaO	Na ₂ O	
<u>ACID LAVAS.</u>										
Microphenocrysts.										
SNb	core	51.20	0.32	0.93	14.33	0.98	11.46	18.92	0.42	98.56
(5 pairs)	rim	51.32	0.20	0.79	13.81	0.99	11.48	19.57	0.42	98.58
SN	core	50.07	0.37	1.09	18.44	0.96	10.37	19.01	0.38	100.69
(4 pairs)	rim	49.53	0.48	1.11	17.27	0.81	10.54	19.49	0.38	99.61
Xenocrysts.										
SNb	core	51.19	0.67	3.34	7.61	0.19	16.12	19.39	0.21	98.72
(4 pairs)	rim	51.26	0.67	3.09	8.30	0.26	16.48	18.81	0.23	99.10
<u>INTERMEDIATE TEPHRA:</u>										
Xenocrysts:										
N3	core	52.29	0.54	2.47	7.56	0.20	17.36	18.71	0.18	99.31
(4 pairs)	rim	51.56	0.57	2.89	7.33	0.22	16.52	19.70	0.22	99.01
<u>BASALTIC TEPHRA.</u>										
Microphenocrysts.										
Lj2	core	51.05	0.88	3.71	7.96	0.23	15.62	19.41	0.28	99.14
(4 pairs)	rim	51.97	0.52	2.27	7.80	0.23	16.75	19.20	0.19	98.93
S8	core	50.65	0.59	3.73	8.02	0.12	15.54	19.41	0.23	98.29
(2 pairs)	rim	52.15	0.41	2.58	7.83	0.11	17.01	19.40	0.23	99.72
S1	core	50.13	1.25	4.11	10.11	0.17	14.48	18.53	0.29	99.07
(1 pair)	rim	52.35	0.51	1.85	9.06	0.29	16.25	18.93	0.23	99.44
VE1	core	51.09	0.67	3.31	7.33	0.19	16.63	19.50	0.20	98.92
(7 pairs)	rim	51.11	0.72	3.21	8.00	0.18	16.78	18.71	0.20	98.90
Xenocryst in Stutshraun lava.										
SH2	core	51.32	0.24	0.97	12.29	0.76	12.56	20.03	0.50	98.67
	rim	50.54	0.73	2.44	8.87	0.28	15.81	19.65	0.24	98.56

Table 3. Clinopyroxene compositions. Mean values of core and rims to illustrate the zoning in some selected samples.

OLIVINE.								
<u>ACID LAVAS.</u>		<u>FO</u>	<u>SiO₂</u>	FeO	MnO	MgO	CaO	
Microphenocryst.								
NH9	core	19.9	30.48	59.33	2.02	8.27		100.10
(1 pair)	rim	21.6	31.11	56.27	1.95	8.70		98.03
Xenocrysts.								
NH3	core	76.8	38.74	21.37	0.50	39.77	0.09	100.47
(1 pair)	rim	71.7	37.93	25.56	0.60	36.40	0.11	100.60
L5	core	76.8	38.67	20.90	0.32	38.85	0.08	98.82
(2 pairs)	rim	76.5	39.02	21.08	0.37	38.37	0.07	98.91
INTERMEDIATE TEPHRA.								
Xenocrysts.								
N3	core	74.1	38.89	22.87	0.46	36.75	0.10	99.07
(1 pair)	rim	69.2	38.03	27.02	0.41	33.97	0.02	99.45
S5b(1)	core	72.5	38.05	24.84	0.47	36.77	0.03	100.16
(1 pair)	rim	71.8	38.19	25.30	0.40	36.24	0.12	100.25
BASALTIC TEPHRA.								
Microphenocrysts.								
VE1	core	78.4	38.54	19.98	0.31	40.66	0.31	99.80
(4 pairs)	rim	78.6	38.71	19.75	0.31	40.63	0.33	99.73
Lj2	core	76.9	38.56	20.98	0.29	38.95	0.09	98.87
(2 pairs)	rim	76.1	38.70	21.69	0.39	38.77	0.12	99.67
S8	core	77.6	38.78	20.47	0.18	38.46	0.10	97.99
(1 pair)	rim	77.8	38.56	21.06	0.32	40.01	0.06	100.01
Phenocryst in Stutshraun lava.								
SH2	core	68.5	37.12	27.77	0.39	33.94	0.30	99.52
(1 pair)	rim	64.5	36.27	31.15	0.60	31.79	0.30	100.11

Table 4. Mean values of core and rim compositions of olivine from some selected samples.

	Fisk et al. (1978)	Roeder & Emslie (1970)	Roeder (1974)	Leeman & Scheidegger (1977)
VE1	1132 - 1137	1172 - 1176	1166 - 1170	1177
Lj2	1100 - 1107	1144 - 1150	1136 - 1142	1154 - 1157
S8	1146 - 1156	1184 - 1193	1179 - 1188	1194 - 1205

Table 5a. Temperatures (°C) based on MgO_{ol}/MgO_{liq} for basaltic tephra.

	Calculated cpx-composition			CPX _{calc} /melt	CPX _{anal} /melt
	En	Fs	Wo	T (°C)	T (°C)
VE1	47.4	12.8	39.8	1149	1158
Lj2	46.6	15.0	38.4	1124	1139
S8	48.7	13.8	37.6	1143	1153

Table 5b. Clinopyroxene compositions and temperatures of basaltic tephra calculated from melt compositions by the iteration procedure of Nielsen & Drake (1979). Predicted temperatures are compared with analysed clinopyroxene-melt values.

	P_{H_2O}	0	500 bars	1000 bars	5000 bars
NH9	T (°C)	924 - 1048	877 - 995	1809 - 941	765 - 812

Table 5c. Temperature - P_{H_2O} relations for the NH9 rhyolitic lava sample. Based on 8 plagioclase crystals. (Method of Kudo & Weill (1970)).